Revised Classification of the Righteye Flounders (Teleostei: Pleuronectidae) Based on Multilocus Phylogeny with Complete Taxon Sampling

Kirill A. Vinnikov[a,b*], Robert C. Thomson[a], and Thomas A. Munroe[c]

[a] *Department of Biology, University of Hawai'i at Mānoa, Honolulu, HI 96822, USA*

[b] *Department of Marine Biodiversity and Bioresources, Far Eastern Federal University, Vladivostok, 690091, Russia*

[c] *National Systematics Laboratory, NOAA's National Marine Fisheries Service, Office of Science and Technology, National Museum of Natural History, Smithsonian Institution, Washington, DC 20013, USA*

[*] Corresponding author at: Department of Biology, University of Hawai'i at Mānoa, 2538 McCarthy Mall, Edmondson 216, Honolulu, HI 96822, USA

E-mail address: vinni@hawaii.edu (K.A. Vinnikov)

Abstract

Members of the family Pleuronectidae are common representatives of the marine benthic fauna inhabiting northern regions of the Atlantic and Pacific oceans. The most recent comprehensive classification of the family, based entirely on morphological synapomorphies, recognized five subfamilies, 23 genera, and 61 extant species. However, several subsequent molecular studies have shown that many synapomorphic characters discovered in the morphological study might represent homoplasies, thereby questioning the reliance on these characters with the warning that they may provide misleading information for testing other morphology-based evolutionary hypotheses. In the present study, we propose a comprehensive taxonomic reassessment of the family Pleuronectidae based on the molecular phylogeny reconstructed from four nuclear and three mitochondrial loci and represented by complete taxon sampling of all but one valid species currently assigned to this family. To check for robustness of the phylogenetic hypothesis, we analyzed the effect of base compositional heterogeneity on phylogenetic signal for each gene and compared six different gene partitioning schemes. The final dataset, comprising 14 partitions and 154 individuals, was used to reconstruct phylogenetic trees in RAxML, MrBayes and BEAST2. Alternative topologies for several questionable nodes were compared using Bayes factors. The topology with the highest marginal likelihood was selected as the final phylogenetic tree for inferring pleuronectid relationships and character evolution. Based on our results, we recognize the Pleuronectidae comprising 5 subfamilies, 24 genera and 59 species. Our new phylogeny comprises five major monophyletic groups within the family, which we define as the subfamilies within the family: Atheresthinae, Pleuronichthyinae, Microstominae, Hippoglossinae and Pleuronectinae. Taxonomic composition of most of these subfamilies is different from that proposed in previous classifications. We also re-assess hypotheses proposed in earlier studies regarding intra-relationships of species of each lineage. Results of the current study contribute to better understanding of the evolutionary relationships of pleuronectid flatfishes based on molecular evidence, and they also provide the framework towards future comprehensive morphological revision of constituent lineages within the family Pleuronectidae.

Keywords:

flatfish systematics, character reassessment, synapomorphies, species tree, MrBayes, BEAST2, StarBEAST, stepping stone analysis, Bayes factors, compositional heterogeneity

1. Introduction

Due to high commercial value of the majority of its species, their relatively large size and close proximity to researchers studying these fishes, the family Pleuronectidae represents the best studied group of flatfishes within the order Pleuronectiformes. However, despite the long historical interest in these fishes, their systematics remains controversial primarily due to many alternative hypotheses that have been proposed for their classification, and also because of questions regarding taxonomic validity of some pleuronectid species. Throughout the 20th century, the number of subfamilies, genera and species considered as valid, as well as their phylogenetic relationships, have changed repeatedly (Table S1). The most recent classification of the family Pleuronectidae represents an ad hoc hypothesis of relationships constructed from the literature and includes five subfamilies, 23 genera and 61 species (Table S1; Nelson et al., 2016).

Historically (Cuvier, 1816; Jordan and Goss, 1889), the Pleuronectidae was the family that included all known species of flatfishes. In his monumental revision of flatfishes, Norman (1934) recognized five families of flatfishes, including the Pleuronectidae. In this work, five subfamilies were proposed within the Pleuronectidae: Pleuronectinae, Paralichthodinae, Poecilopsettinae, Rhombosoleinae and Samarinae. All of these subfamilies were later raised to family level (Chapleau and Keast, 1988). Subsequently, Cooper and Chapleau (1998) revised the classification of the Pleuronectidae (sensu Chapleau and Keast, 1988) proposing five subfamilies: Hippoglossinae, Eopsettinae, Lyopsettinae, Hippoglossoidinae and Pleuronectinae, based on their cladistic analysis of 106 morphological characters. They also divided the Pleuronectinae into four tribes: Psettichthyini, Isopsettini, Microstomini and Pleuronectini. Cooper and Chapleau (1998) provided the first evidence for family monophyly based on morphological characters, including 10 family synapomorphies. Their study, comprising the majority of valid species, resulted in the first comprehensive phylogenetic hypothesis for the family Pleuronectidae. However, some taxonomic changes proposed by Cooper and Chapleau (1998) have not been supported by subsequent studies (Orr and Matarese, 2000; Suzuki et al., 2001), and the taxonomic status of several genera (e.g., *Embassichthys, Limanda*, *Liopsetta*, *Pleuronectes*) remains unclear.

The monophyly of the family Pleuronectidae has been supported in many molecular studies (Berendzen and Dimmick, 2002; Kartavtsev et al., 2007; Roje, 2010; Betancur-R et al., 2013a; Ji et al., 2016). However, all of those phylogenetic analyses included only a subset of the pleuronectid species, which, in turn, were represented by only a single, or just a few individuals. Such limited sampling

usually precludes any strongly supported inference about taxonomy and can lead to erroneous conclusions. For instance, Kartavtsev et al. (2007) proposed the synonymy of *Hippoglossoides elassodon* and *H. robustus* and of *Pseudopleuronectes yokohamae* and *P. schrenki* because they observed only small genetic distances within each corresponding pair of species. However, all voucher samples used in that phylogenetic study were collected in geographic regions not representative of type localities of either species within a pair, which raises the possibilities of their misidentification. Conversely, Roje (2010) performed the most comprehensive molecular analysis of phylogenetic relationships among pleuronectid species and incorporated species differences in larval morphology in her study. Her results showed significant branch support for recognizing separate lineages for both *Hippoglossoides elassodon* and *H. robustus* and for inferring that both species are valid taxa.

Roje's (2010) phylogenetic and ancestral state reconstruction analyses also revealed a similar general trend in jaw evolution within the Pleuronectidae as was previously hypothesized by Cooper and Chapleau (1998). Results from both studies indicate evolution from lineages with large symmetrical jaws and numerous multiserial teeth to lineages with small asymmetrical jaws and a few uniserial teeth. Despite similarities observed in jaw evolution between these studies, comparison of the morphological and molecular phylogenies exposed several substantial discrepancies (Fig. S1), raising serious concerns about interpretation of some morphological characters as synapomorphies by Cooper and Chapleau (1998). For example, the genus *Atheresthes*, which was previously synonymized with *Reinhardtius* by Cooper and Chapleau (1998), appears as a monophyletic genus distinct from the latter on Roje's molecular tree. Moreover, it was shown as the earliest diverging group on the pleuronectid molecular phylogeny (Roje, 2010). Roje (2010) also noted that the genera *Pleuronectes* and *Limanda* (sensu Cooper and Chapleau, 1998) are polyphyletic. However, due to incomplete taxon sampling within both genera, Roje (2010) was unable to provide any further details to support their taxonomic revision.

In addition to the above-mentioned issues, the majority of published molecular-based and morphology-based phylogenetic trees for pleuronectid species contain polytomies and nodes with low statistical support. Therefore, some taxonomic conclusions proposed in those studies require additional verification. Nevertheless, despite these limitations, most existing flatfish phylogenies show strong evidence that the family Paralichthyidae, excluding the "*Cyclopsetta* group" (sensu Betancur-R et al., 2017), is sister to the family Pleuronectidae (Betancur-R et al., 2013ab; Campbell et al., 2014; Harington et al., 2016). These two families are remarkably different from each other in morphology. Many species within Paralichthyidae have a large mouth and all usually have their eyes located on the left side of the

head in adults (Norman, 1934). In contrast, most pleuronectid species have small mouths, and, with a singular exception (the intraspecific form of starry flounder, *P. stellatus*), have their eyes on the right side, the feature by which they are known as "righteye" flounders.

In the current study, we provide the first molecular-based phylogenetic hypothesis including almost the entire assemblage of species currently assigned to the family Pleuronectidae (60 of the total of 61 valid species). This new taxonomic reassessment of the family Pleuronectidae is based on the general lineage concept of species (de Queiroz, 1998), where we recognize lineages using phylogenetic criteria (Cracraft, 1983). To avoid possibilities of erroneous species identifications, we attempted to represent each species by including several museum topotypes – voucher specimens that were collected in proximity to each type locality for the individual species. This sampling approach was deemed especially important for those taxa whose validity was questionable. We reconstructed the phylogenetic trees with maximum likelihood (ML) and Bayesian methods, incorporating multiple nuclear and mitochondrial loci. Using the resulting phylogeny, we: (1) reassessed the phylogenetic information of some morphological characters studied in the previous hypotheses; and (2) provided a new and revised classification of the family Pleuronectidae.

2. Materials and methods

2.1. Specimen and taxon sampling

We collected muscle and fin tissue samples from 144 individuals, representing 60 of 61 valid species from the family Pleuronectidae. The ocellated turbot, *P. ocellatus*, was the only pleuronectid species for which samples were not included in the current study. Additionally, we used 6 individuals of 5 species from the family Paralichthyidae as the outgroup for phylogenetic analyses. All tissue samples were obtained from specimens curated in different museum collections, and for most cases, where voucher specimens were available for morphological comparisons (Table S2). To increase sample representation of *H. hippoglossus*, *L. limanda*, *M. kitt* and *P. platessa*, we also obtained DNA sequences of voucher specimens of these species from NCBI GenBank (Benson et al., 2017). These data constituted less than 1% of the total number of sequences produced in this study (Table S2). To adequately represent each questionable or recently described species (e.g., *C. herzensteini*, *C. pinetorum*, *H. elassodon*, *H. robustus*, *L. polyxystra*, *M. shuntovi*, *P. japonicus*, *P. schrenki*), several voucher specimens, identified according to diagnostic features provided in their original morphological descriptions and collected in the type locality of each species, were examined by one of the authors (KV). For species with widespread distributions (e.g., *C. asperrimum*, *L. aspera*, *P. stellatus*), we used at least several individuals collected from distant parts of their geographic ranges in order to estimate divergence between potentially isolated populations within these species.

2.2. DNA extraction, amplification, sequencing and alignment

DNA was extracted from tissue samples using Qiagen DNeasy Blood & Tissue Kit according to the manufacturer's protocol (Qiagen, Valencia, CA). We used GoTaq® Hot Start Green Master Mix (Promega, Madison, WI) to amplify two complete mitochondrial genes, cytochrome oxidase subunit I (*COI*, 1548 bp) and cytochrome b (*cytb*, 1141 bp) with the partial region of threonyl-tRNA (*tRNA-Thr*, 79 bp); exonic regions of three nuclear genes, recombination-activating gene 1 (*RAG1*, 798 bp), recombination-activating gene 2 (*RAG2*, 861 bp), rhodopsin gene (*Rho*, 1062 bp with indels) and partial untranslated region from 3' end in rhodopsin gene (*Rho-UTR*, 254 bp with indels), resulting in 5,743 bp of total sequence size. Primers for amplification and sequencing (Table S3) were designed in Primer3 (Untergasser et al., 2012) and manufactured by IDT. Source templates for primer design and primer parameter estimations were prepared based on all Carangaria (sensu Betancur-R et al., 2017) nucleotide sequence records retrieved from NCBI GenBank (Benson et al., 2017) and aligned in MUSCLE (Edgar,

153 2004). Each amplification was conducted in 25 µL reaction mix containing 1µL of 50 ng/µL template
154 DNA, 0.3 µL of each 10 µM upstream and downstream primers, 12.5 µL of GoTaq® Green Master Mix
155 (2X) and 10.9 µL of nuclease-free water. The polymerase chain reaction consisted of the following
156 steps: initial denaturation at 95ºC for 3 min; 35 cycles of 40 s at 95ºC, 40 s at the primer-specific
157 annealing temperature (Table S3), and 90 s at 72ºC; with final extension at 72ºC for 5 min.
158 Amplification products were screened in 1.5% agarose gel electrophoresis and purified with USB
159 ExoSAP-IT following the manufacturer's protocol (Affymetrix, Santa Clara, CA). Sequencing was
160 performed on ABI 3130XL Genetic Analyzer (Applied Biosystems, Waltham, MA) at Biotech Core
161 (Pacific Biosciences Research Center, University of Hawaii at Manoa, Honolulu, HI). Resulting
162 nucleotide sequences were manually corrected and assembled for each amplification product in
163 Geneious 6.1 (http://www.geneious.com, Kearse et al., 2012), and then all gene sequences were aligned
164 using MUSCLE (Edgar, 2004). Sequence concatenations and file format conversions were implemented
165 in SequenceMatrix (Vaidya et al., 2011).

166 *2.3. Partitioning scheme and model selection*

167 We used different partitioning strategies in order to find the best-fitted combination of nucleotide
168 substitution model parameters for each subset of data. Protein coding sequences of *COI*, *cytb*, *RAG1*,
169 *RAG2* and *Rho* were initially partitioned based on three codon positions and, together with *tRNA-Thr*
170 and *Rho-UTR*, they produced 17 partitions in total. Optimal partitioning schemes were chosen by the
171 'greedy' heuristic search algorithm in PartitionFinder 1.1.1 (Lanfear et al., 2012) with the
172 implementation of either Akaike Information Criterion (AIC; Akaike, 1973) or Bayesian Information
173 Criterion (BIC; Schwarz, 1978). Additionally, we manually introduced four partitioning schemes that
174 represented either the dataset with the maximum number of partitions (17 partitions), all sequenced
175 coding and non-coding regions (7 partitions), subsets of mitochondrial and nuclear genomes (2
176 partitions) or the total evidence (1 partition). We estimated the best-fitting nucleotide substitution model
177 for each partition using the maximum likelihood approach implemented in jModelTest 2.1.10 (Darriba
178 et al., 2012) and in PartitionFinder 1.1.1 (Lanfear et al., 2012).

179 To select the optimal set of model parameters and corresponding phylogenetic tree, we compared
180 all partitioning schemes using the likelihood ratio test (Wilks, 1938) for the ML trees and Bayes factors
181 (Kass and Raftery, 1995) for the Bayesian trees. Bayes factors (BF) were computed from the marginal
182 likelihoods using Stepping Stone (SS) analysis (Fan et al., 2011; Xie et al., 2011). The latter method

samples from a series of power posterior distributions that represent a gradual transformation of the joint posterior to the joint prior distribution, controlled by parameter β. For all stepping stone analyses in MrBayes (Ronquist et al., 2012), we performed two MCMC runs with 6 chains and 100 steps of 500,000 generations each, sampling every 100th generation and discarding 1000 samples at the beginning of each step as burnin. The final marginal log-likelihood value for each run was obtained by path sampling estimation using 'sumss' command. Each log BF was calculated as the difference between log marginal likelihoods for each model and considered as strong evidence for a candidate model if its value was greater than 10 (Kass and Raftery, 1995).

2.4. Phylogenetic tree inference

Phylogenetic trees were reconstructed with maximum likelihood and Bayesian approaches. All procedures were implemented on the CIPRES Science Gateway portal (Miller et al., 2015). For each gene and for each concatenated dataset, we performed 200 alternative runs on distinct starting trees with the rapid hill-climbing algorithm in RAxML (Stamatakis, 2014), assigning GTR+G substitution model for every partition, and chose the tree with the maximum likelihood value (ML tree). Node support values were obtained from 1000 iterations of non-parametric bootstrap and mapped onto the ML tree. Bayesian trees were reconstructed with the Markov Chain Monte Carlo (MCMC) sampling procedure implemented in MrBayes 3.2.6 (Ronquist et al., 2012). We used two independent runs with 6 chains (1 cold and 5 heated) and 15 million generations, sampling every 500th generation from a cold chain and disregarding the first 20% of samples as burnin. Model and prior distribution settings for each partition were set according to the best-fitting nucleotide substitution models. If the selected substitution model was not incorporated in MrBayes software, we used the closest one with a higher complexity. The convergence between MCMC runs, distributions of marginal likelihood parameter estimates, their effective sample sizes, and the uniformity of sampling traces were analyzed in Tracer 1.6.1 (Rambaut et al., 2014). All phylogenetic trees were visualized in *ape* v.3.5 (Paradis et al., 2004) and *phytools* v.05-38 (Revell, 2012) packages in R (R Core Team, 2016).

2.5. Stepping stone analysis of topology

We considered several nodes with weak support on the final Bayesian tree as alternative hypotheses of pleuronectid relationships. To test these different tree topologies, we compared their log BF estimated with SS analysis under fixed topology prior and the best fitted partitioning scheme. We

used the same settings for MCMC runs as we applied for selecting the best-fitted partitioning scheme (see details above).

2.6. Phylogenetic bias in gene trees

Particular genes can provide strongly biased phylogenetic signal due to high levels of their base compositional heterogeneity. We measured this effect in our study by comparing compositional heterogeneity of each locus against its phylogenetic signal. Gene trees were reconstructed with the maximum likelihood approach (see details above). The phylogenetic informativeness of each gene tree was estimated in two different ways: by averaging bootstrap values across all internal nodes and by measuring topological distances (Penny and Hendy, 1985) between the gene tree and the ML tree derived from the concatenated dataset where each locus was considered as a separate partition. Both metrics were computed using the *ape* v.3.5 package in R (Paradis et al., 2004; R Core Team, 2016). Base compositional heterogeneity of each locus was estimated by χ^2 test implemented in PAUP v.4.0a150 (Swofford, 2002), by averaged disparity indices (I_D; Kumar and Gadagkar, 2001) calculated in MEGA v.7.0.16 (Kumar et al., 2016), and by observing deviations in GC content. Following the strategy described in Betancur-R et al. (2013a), we observed the effect of non-stationarity on the phylogeny by testing correlations between the estimates of base compositional heterogeneity and phylogenetic signals in all loci.

2.7. Species tree inference

We used StarBeast (*BEAST), a default package in BEAST v.2.4.3 (BEAST 2), as a Bayesian approach for inferring gene trees and a shared species tree under the multispecies coalescent model (Heled and Drummond, 2010; Bouckaert et al., 2014). The best-fitted substitution model for each partition was selected from a total of 56 models in jModelTest (Darriba et al., 2012). We unlinked the substitution and tree model for all loci, except for the mitochondrial loci (which had independent substitution models but a shared tree model). We ran three independent MCMC analyses with 300 million generations each, sampling every 10,000 generations and discarding the first 30 million generations as burnin. Chain convergence and effective sample sizes for all model parameters were observed in Tracer 1.6.1 (Rambaut et al., 2014). The resulting species trees were processed and visualized in DensiTree (Bouckaert, 2010). Additionally, we compared the results of *BEAST analysis with a summary coalescent method implemented in ASTRAL-II (Mirarab and Warnow, 2015), using the

241 RAxML tree for each partition as input data for species tree reconstruction. In both *BEAST and
242 ASTRAL-II analyses, we used multiple individuals per species, excluding the outgroup taxa.

243 *2.8. Ancestral character state reconstruction*

244 The ancestral state reconstructions of the quantitative characters (e.g., numbers of abdominal and
245 caudal vertebrae) on the species molecular tree were implemented in *phytools* v.05-38 package in R
246 (Revel, 2012; R Core Team, 2016) using the maximum likelihood approach (Felsenstein, 1985).
247 Morphological data for all extant species were obtained from the personal examination of voucher and
248 other museum specimens, including X-ray imaging, and from the literature sources (Norman, 1934;
249 Sakamoto, 1984; Cooper and Chapleau, 1998; Voronina, 2002, 2005). For each ancestral node estimate,
250 we computed 95% confidence interval. Correlations between states of different characters were tested
251 with phylogenetic independent contrasts (Felsenstein, 1985). Then this information was used for
252 identification of morphological synapomorphies for selected monophyletic groups on the pleuronectid
253 phylogeny.

3. Results

3.1. Sequencing and alignment

In our study, we used nucleotide sequences ranging in size from 708 to 1548 bp for five protein coding regions, 79 bp for the *tRNA-Thr* coding gene, and 254 bp for untranslated region in the *Rho* gene (Table 1). All sequences used in the analysis were submitted to NCBI nucleotide database (Table S2). The final dataset of 154 individuals and 7 loci was more than 99% complete. Short gaps in the alignment were accepted as indels and, therefore, were retained in the final sequence matrix. The proportion of variable sites was different between loci, ranging from 29% in the *RAG1* gene to 54% in the *cytb* gene (Table 1). The length of the *COI* gene varied across species due to a few additional codons located close to the 3' end. Hence, we decided to trim the *COI* alignment by the length of the shortest sequence.

3.2. Partitioning scheme and model selection

We created a pool of candidate partitioning schemes that we compared using maximum likelihood and Bayesian approaches in order to choose a set of models for the final phylogenetic tree inference (Table 2). Two of these partitioning schemes were proposed a posteriori by PartitionFinder (Lanfear et al., 2012) based on AIC and BIC, while the rest of the schemes were defined a priori following different hierarchies of the genetic code structure (Table 2). Marginal likelihoods estimated via stepping stone sampling supported the scheme with 14 partitions (-56531.37; Table 2). In all stepping stone analyses, we used several independent MCMC sampling runs, which converged successfully and resulted in high effective sample sizes for all parameter estimates (ESS>>200). The Bayes factors (BF) revealed strong evidence in favor of the best supported partitioning scheme by showing a 100X magnitude of difference with the next closest model (log BF = -291.52; Table 2). Thus, we accepted the phylogeny of the Bayesian tree reconstructed from the dataset with 14 partitions (hereafter referred to as the BA tree) and the nucleotide substitution models selected for each partition in PartitionFinder with AIC.

3.3. Phylogenetic tree inference

The molecular phylogeny on the BA tree reveals five major monophyletic groups, a classification that only partially reflects previous hypotheses regarding the taxonomy of righteye flounders (Fig. 1). The genus *Atheresthes*, including two sister species, *A. stomias* and *A. evermanni*, was recovered as a sister group (Group I in Fig. 1) to the rest of the pleuronectids. The second major monophyletic group (Group II in Fig. 1) comprises a single genus, *Pleuronichthys* (sensu Cooper and Chapleau, 1998),

represented by seven valid species, including the just recently revised *P. cornutus* and *P. lighti*. Noteworthy is that all branch lengths in this group were extremely long in comparison with those for the majority of species on the tree.

The third major monophyletic group corresponds in part to the tribe Microstomini of previous classifications (Table S1) with inclusion of several genera: *Embassichthys*, *Glyptocephalus* and *Microstomus* (Group III in Fig. 1), previously classified in this group. All four species from the monophyletic *Glyptocephalus* were highly distinct. The monophyletic sister group to this clade includes the genera *Microstomus* and the monotypic *Embassichthys*, whose relationships were not fully resolved, resulting in the only polytomy present on the BA tree. The relatively low Bayesian posterior probability (BPP) for the clade with the species, *M. pacificus*, also indicated some uncertainty regarding relationships of this species with its congeners.

The fourth major monophyletic group (Group IV in Fig. 1) includes all species from the subfamilies Hippoglossinae (excluding the genus *Atheresthes*), Eopsettinae and Lyopsettinae. Most internal nodes in this group have moderate or low support ($0.8 < BPP \leq 1$). Two monotypic genera, *Lyopsetta* and *Clidoderma*, were recovered as sister taxa, with both having very long branches (BPP = 0.97). Their clade was sister to the clade containing the genus *Eopsetta*, including two distinct species, *E. grigorjewi* and *E. jordani* (BPP = 0.97), and the rest of the Hippoglossinae species (BPP = 1). Relationships among *Hippoglossus*, *Reinhardtius* and *Verasper* were poorly supported (BPP = 0.81–0.84).

The fifth major monophyletic group (Group V in Fig. 1) includes the remainder of the species of the Pleuronectidae. Relationships among species belonging to this clade were fully resolved. Group V was subdivided into two large sister monophyletic groups, one of which encompasses all species from the subfamily Hippoglossoidinae (sensu Nelson et al., 2016) plus the monotypic *Dexistes* and three species from the genus *Limanda*: *L. aspera*, *L. limanda* and *L. sakhalinensis*.

As previously noted by Roje (2010), the genera, *Limanda* and *Pleuronectes*, are polyphyletic. Our results agree with this hypothesis as three other species previously classified in the genus *Limanda* (*L. ferruginea*, *L. proboscidea*, and *L. punctatissima*) are deeply nested within a different monophyletic group in our pleuronectid phylogeny. Additionally, the BA tree shows that *L. punctatissima* does not share the most recent common ancestry (MRCA) with its congeneric species, *L. ferruginea* and *L. proboscidea* (BPP = 0.95; Fig. 1). Similarly, two species from *Pleuronectes, P. platessa and P.*

313 *quadrituberculatus,* do not share their MRCA with the other congeneric species, previously considered
314 as a valid genus *Liopsetta* (Table S1; Evseenko, 2004). *Hippoglossoides* was represented by a
315 monophyletic group that includes *H. platessoides* as the basal taxon and three other species, *H. dubius,*
316 *H. elassodon*, *H. robustus*, having unresolved relationships (Fig. 1). Another interesting result is that
317 *Cleisthenes herzensteini* and *C. pinnetorum*, previously recognized as distinct species, are not
318 distinguished by the genetic approaches we employed in our phylogenetic study (Fig. 1). We also found
319 that the monophyly of each tribe within the subfamily Pleuronectinae, proposed by Cooper and
320 Chapleau (1998) and accepted by Nelson et al. (2016), is not supported by the molecular phylogeny
321 inferred from the BA tree (Fig. 1). Additionally, the BA tree showed significant evidence of a new
322 species within the genus *Platichthys* (Fig. 1).

323 Besides performing several independent runs in MrBayes (Ronquist et al., 2012), we repeated the
324 phylogenetic tree reconstruction with the Bayesian approach in BEAST 2 (Bouckaert et al., 2014) to
325 confirm the consistency of the inferred phylogeny. We applied the same nucleotide substitution model
326 settings as we used for the phylogenetic analysis in MrBayes (see above) and an uncorrelated lognormal
327 clock model (UCLN; Drummond et al., 2006) was employed, which has been used previously as a
328 potentially appropriate clock model for ray-finned fish evolution (Near et al., 2012; Betancur-R et al.,
329 2013b). The BEAST tree exposed several discrepancies with the BA tree (Fig. S2). It showed significant
330 support for *H. dubius* (BPP = 1.0), which shared a common ancestry with the monophyletic group
331 consisting of *H. elassodon* and *H. robustus*, which, in turn, were clustered geographically rather than by
332 species affinity (BPP = 0.98, Fig. 2). *Embassichthys bathybius* was recovered as sister lineage to the
333 genus *Microstomus* (BPP = 1). BEAST analysis also recognized the same five major monophyletic
334 groups as were identified on the BA tree (Fig. S2). However, some well supported nodes from the BA
335 tree showed relatively low support on the BEAST tree (Fig. S2). For example, the BEAST tree revealed
336 much higher uncertainty for the phylogenetic relationships among the genera within Group IV and for
337 the branch with *L. punctatissima* (Fig. S2). Groups III and IV were shown as sister monophyletic groups
338 on the BEAST tree (BPP = 0.99), and the branch support for Group II was low (BPP = 0.65; Fig. S2).

339 *3.4. Stepping stone analysis of topology*

340 Comparison of the BA and the BEAST trees has shown that the recovered topology still requires
341 some additional verification. We tested four alternative topological hypotheses by setting fixed topology
342 prior in each SS analysis (Fig. 3). In order to resolve the polytomy, we manually modified the original

BA tree by creating the node with the lineage containing *E. bathybius* and making it sister to the '*Microstomus*' monophyletic group, similar to the topology that was revealed for the BEAST tree (Fig. S2). Additionally, we grouped *L. punctatissima* together with its congeneric species, *L. ferruginea* and *L. proboscidea,* without any impact on their branch lengths. The rationale for making these two changes emerged from the strong morphological evidence provided by Norman (1934) and Cooper and Chapleau (1998). The SS analysis indicated that these tree modifications did not cause any substantial deviations in the marginal likelihood estimations (log BF = -2.57; Fig. 3A). After swapping the monophyletic groups with the genera *Verasper* and *Reinhardtius,* we observed a slightly greater difference in marginal likelihoods (log BF = -4.23; Fig. 3B). The topology, where Group III (aka 'Microstominae') and Group IV (aka 'Hippoglossinae') shared the MRCA, has more substantial change in marginal likelihood estimates (log BF = -5.50; Fig. 3C), which became even more severe when we combined all three modifications in a single topology (log BF = -7.3; Fig. 3D). All these deviations in the log marginal likelihood estimates do not strongly favor any alternative topological hypothesis we had tested. Thus, for the following inference of morphological character evolution and taxonomic revision of the family Pleuronectidae, we decided to use the original topology (Fig. 3A), in which we made only two changes: placing *L. punctatissima* within the monophyletic group including *L. ferruginea* and *L. proboscidea*, and by resolving the polytomy in the genus *Microstomus*.

3.5. Phylogenetic bias in gene trees

The GC content varied between loci and was substantially lower for the mitochondrial (0.46–0.47; Table 1) compared to the nuclear protein coding regions (0.51–0.58; Table 1). The lowest average GC score was observed for untranslated region in *Rho* gene. Additionally, we used disparity index and χ^2 score for estimating the base compositional heterogeneity at each locus. Estimates for both metrics showed a strong positive correlation (R^2 = 0.9116, p = 0.0008; Fig. S3A).

The phylogenetic signal of each locus was estimated from the corresponding RAxML tree (Fig. 4A). For each tree, we averaged the bootstrap values across all internal nodes and measured its topological distance from the ML tree (Fig. S4) derived from the concatenated dataset with each locus treated as a separate partition (Table 1). The highest phylogenetic signal was obtained from the mitochondrial *COI* and *cytb* genes, which also had the largest lengths and proportions of variable sites among all protein coding genes used in the current study (Table 1). Despite their relatively high informativeness and shared evolutionary history, all mitochondrial loci produced different topologies

373 (Fig. 4A). Both approaches used for testing phylogenetic signal revealed strong negative correlation in
374 their estimates (R^2 = 0.8799, p = 0.0018; Fig. S3B), confirming their consistency and allowing us to
375 employ just one measure in the following comparisons.

376 Although no clear effect of sequence size on base heterogeneity was evident (R^2 = 0.3082, p =
377 0.1958; Fig. S3C), alignment length had a strong explanatory power for phylogenetic signal (R^2 =
378 0.9077, p = 0.0009; Fig. S3D). Finally, we did not observe a substantial effect of a compositional
379 heterogeneity on a phylogenetic signal (R^2 = 0.3197, p = 0.1859). Moreover, the revealed relationship
380 between the disparity indices and the topological distances was quite opposite to what would be
381 expected if there was a case of any significant bias in a phylogenetic signal (Fig. S3E), however, the
382 number of compared loci was very small (n = 7).

383 Despite their differences in phylogenetic signal, all loci used in the current study independently
384 unveiled serious discrepancies in the current taxonomy and systematics of the family Pleuronectidae
385 (Fig. 4A). The majority of previously accepted subfamilies (Table S1) were revealed as polyphyletic
386 across all RAxML tree topologies, with exception of the Eopsettinae, having only two species, and also
387 the monotypic Lyopsettinae. On most trees, the latter two subfamilies were grouped together with the
388 Hippoglossinae (sensu Nelson et al., 2016). The tribe Pleuronectini was recognized as a paraphyletic
389 group because the other two other tribes, Psettichthyini and Isopsettini, were nested within its clade (Fig.
390 4A).

391 Both nuclear and mitochondrial protein-coding gene trees were highly consistent in revealing
392 similar clades, which correspond with the major monophyletic groups on the BA tree (Fig. 4A). The
393 genus *Atheresthes* was shown as the sister lineage to the remaining pleuronectids on all gene trees, and
394 this placement has also been recovered in previous studies (Berendzen and Dimmick, 2002; Roje, 2010).
395 Within the group of remaining pleuronectids, the clade containing the genus *Pleuronichthys* (sensu
396 Cooper and Chapleau, 1998) represented the first divergence making it a sister group to all other taxa.
397 This result was also consistent across all loci. However, many conflicting nodes were observed between
398 the gene trees. For example, phylogenetic relationships among species of the clades Hippoglossinae and
399 Microstomini were not congruent across different gene topologies, and often these hypothesized
400 relationships had very low bootstrap support for shifting branches between the gene trees.

401 *3.6. Species tree inference*

Species trees reconstructed in *BEAST and in ASTRAL-II could not resolve the topological ambiguity within the fourth major monophyletic group and its certain position on the tree, but they did show high consistency between each other for the remaining monophyletic groups (Fig. 4B, S5). Both trees agreed that the current classification of the family Pleuronectidae does not reflect the phylogenetic relationships of its species (Fig. 4B, S6). Moreover, they both supported sister relationships of *L. punctatissima* with *L. ferruginea* and *L. proboscidea*, which were not recovered on the BA tree.

3.7. Ancestral character state reconstruction

Here were present the results of the ancestral character state reconstruction analysis for numbers of abdominal and caudal vertebrae. These features are consistently preserved in many fossil remains and are often used as taxonomically important characters in flatfish classification (Norman, 1934; Sakamoto, 1984). Consequently, we reconstructed an ultrametric tree in BEAST 2, a priori using the tree with fixed topology representing the species tree (see details above), and then estimated the ancestral states for both of these quantitative traits along the tree edges and at all internal nodes (Fig. 5). Ninety-five percent confidence intervals for each ancestral node estimate are provided in Table S4. The character state reconstruction analysis revealed rapid evolutionary changes, including several reversals, in the number of vertebrae among the ancestral nodes (Fig. 5). Noteworthy is that the shifts in ancestral states of abdominal vertebrae in most cases coincide with those of caudal vertebrae (Fig. S7). In general, our analysis showed that there is a common trend in the evolution of pleuronectids towards a smaller number of abdominal vertebrae (Fig. 5).

In our phylogenetic reconstructions we confirmed an evolutionary change from a large and symmetric jaw apparatus with multiple rows of teeth on premaxillaries (major monophyletic groups I–IV) towards a much smaller and asymmetric mouth with a single row of dentition on the upper jaw and strongly reduced number of teeth from the ocular side (major monophyletic group V). Additionally, we detected several newly derived morphological character states in some monophyletic groups on the species tree. Major monophyletic groups II–V (node 2 on Fig. 5) are characterized by having parallel arrangement of olfactory lamellae. Species of the genus *Atheresthes*, representing the first major monophyletic group (node 57 on Fig. 5), have barbed teeth on the pharyngeal arch and on the jaws with two enlarged canine-like teeth in front. Small slender villiform teeth and the accessory branch of supratemporal canal extending backwards along the dorsal fin and ending at the posterior part of the body are only present in the major monophyletic group II (node 51 on Fig. 5). Similar accessory branch,

but much shorter in length, is present in all species within the clade with *Isopsetta*, *Lepidopsetta*, *Parophrys* and *Psettichthys* (node 18 on Fig. 5) and appears to be a convergent trait. Species within the clade including the genus *Pleuronichthys* (sensu Norman, 1934; node 52 on Fig. 5) have transverse plicae on the inner side of their lips and a high interorbital ridge with strong bony spines or protuberances. The third major monophyletic group (node 43 on Fig. 5) is characterized by having elongated intestine in the posterior body cavity from the ocular side. More information about synapomorphic morphological characters of different monophyletic groups is provided in taxonomic descriptions below.

4. Discussion

4.1. Phylogenetic bias in gene trees

Phylogenetic inference using common models of substitutions can produce strongly biased results if the data have a high level of compositional heterogeneity (Jermiin et al., 2004). The recent recognition of such an effect in flatfish genes (Betancur-R et al., 2013a; Campbell et al., 2013) has shown the necessity to test the stationarity assumption on our dataset before implementing any further phylogenetic analyses. Using similar approaches as described in Betancur-R et al. (2013a), we found that independently evolving genes including in our analysis have very different levels of base compositional heterogeneity (e.g., *cytb, RAG2* and *Rho*; Fig. S3A). Moreover, our results show that the poor resolution of some gene trees is mainly caused by short lengths of their input alignments, associated with a smaller amount of phylogenetic information (Fig. S3D). At the same time, we did not observe an association between the phylogenetic informativeness of a locus and its compositional heterogeneity. Thus, we concluded that non-stationarity had a minor effect on topological discordance between gene trees in our study. We also attempted to mitigate the impact of GC bias in the third codon position by our data partitioning approach. However, the relatively small number of genes that we used still does not allow us to accept the assumption of stationarity with high credibility.

Additionally, we observed some degree of topological variation among the mitochondrial genes used in the current study. This discordance may be caused by systematic error that stems from poor fit of evolutionary models to real sequence data (Richards et al., 2018).

4.2. Robustness of phylogenetic hypothesis

The topology of the Bayesian phylogenetic tree, produced in MrBayes, was highly consistent with the RAxML, BEAST2, *BEAST and ASTRAL trees using the same partitioning and nucleotide substitution models. Only a few conflicting nodes were observed among these trees: 1) within the Hippoglossinae clade; 2) within the *Microstomus* clade; and 3) between the major monophyletic groups that include these two taxa (Fig. 1). Across all trees inferred in the current study, these questionable relationships were either not resolved or had only modest or low support. Likewise, Kartavtsev et al. (2016), on their phylogeny reconstructed from the analysis of *COI* and *cytb* mitochondrial genes, also obtained unresolved relationships between the tribe Microstomini, the subfamily Hippoglossinae and the rest of the species of Pleuronectinae. A similar polytomy was detected in the analysis of *RAG2*, *ND1* and *16S* genes by Roje (2010). In contrast, Betancur-R et al. (2013a) have shown that several species from

Microstomini and Hippoglossinae constitute a single monophyletic group on the maximum likelihood tree reconstructed using 20 nuclear loci. The resolved nodes on their phylogenetic tree, however, showed relatively low support in comparison with other nodes (Betancur-R et al., 2013a). In our study, the Bayes factor analysis did not strongly favor either alternative topology proposed for comparison (log BF = -5.50; Fig. 3C); and therefore, we leave the resolution of these problematic relationships open for future studies.

In general, the resulting phylogeny of our study is well resolved and our data supports the monophyly of the Pleuronectidae. Monophyly of this family had already been revealed in several earlier molecular and morphological studies (Cooper and Chapleau, 1998; Berendzen and Dimmick, 2002; Kartavtsev et al., 2007; Roje, 2010; Betancur-R et al., 2013a). Our new phylogeny also confirms many nodes that previously were less certain because of their poor statistical support. Furthermore, in having almost complete sampling of valid species, our study offers much better representation of the species composition of each genus. This molecular evidence provides strong support for the new taxonomic revision of the family Pleuronectidae.

The final phylogenetic tree (Fig. 1) includes five major monophyletic groups, a hypothesis that does not conform with previous classifications of the family Pleuronectidae (Table S1). These major monophyletic groups were strongly consistent across all trees obtained from independently evolving protein coding regions and between species trees (Fig. 4, S5).

4.3. Morphological evidence for the phylogeny

4.3.1. Major monophyletic group I

The first major monophyletic group is represented by a single genus, *Atheresthes*, and is characterized by: 1) barbed teeth on the jaws and on the pharyngeal arch; 2) a distinct curvature along the ventral margin of the metapterygoid; and 3) a central rachis in the radial olfactory lamellae (Norman, 1934). The latter two character states were identified as plesiomorphic for the family by Cooper and Chapleau (1998). Despite these striking differences between *Atheresthes* and all other species of Pleuronectidae, Cooper and Chapleau (1998) included this genus in the Hippoglossinae (sensu Cooper and Chapleau, 1998), following the results of their cladistic analysis that revealed three morphological synapomorphies: 1) the larger number of abdominal vertebrae; 2) lunate shape of the caudal fin; and 3) a distinct fimbriation on the operculum (Cooper and Chapleau, 1998). However, these three character

499 states can be found across many different flatfish taxa within (Fig. 5) and outside the family
500 Pleuronectidae, and therefore, should be regarded as potentially homoplastic.

501 *4.3.2. Major monophyletic group II*

502 Previously considered as a part of the tribe Microstomini within the Pleuronectinae (Table S1), the
503 genus *Pleuronichthys* makes up the second major monophyletic group on our phylogeny (Fig. 1).
504 *Pleuronichthys* differs from the other genera assigned to the Microstomini by having a very low number
505 of caudal vertebrae (23–25; Fig. 5) and is also characterized in having villiform teeth, an autapomorphy
506 for this genus (Cooper and Chapleau, 1998). Our phylogenetic analysis hypothesizes that all species
507 within *Pleuronichthys* encompass distinct lineages, including the recently revised *P. lighti* and *P.*
508 *cornutus* (Yokogawa et al., 2014). Though not analyzed in the present study, we accept the validity of
509 the ocellated turbot, *P. ocellatus*, based on its unique coloration and morphological features (Norman,
510 1934). Fitch (1963), based on several morphological characters, postulated that *P. ritteri* and *P.*
511 *ocellatus* are sister species. Following his rationale, we hypothesized this sister-relationship in the
512 phylogenetic positioning of *P. ocellatus* on the pleuronectid tree.

513 *4.3.3. Major monophyletic group III*

514 Although phylogenetic relationships between the third and the fourth major monophyletic groups
515 are not well supported in our study, the monophyly of each group is not in doubt. The third major group
516 includes three genera: *Embassichthys*, *Glyptocephalus* and *Microstomus* (sensu Nelson et al., 2016).
517 Supporting results presented in the revision of Cooper and Chapleau (1998), our phylogenetic analysis
518 shows that *Embassichthys bathybius* is closely related to species assigned to the genus *Microstomus*;
519 therefore, we agree with Cooper and Chapleau (1998) that *Embassichthys bathybius* should be
520 transferred to *Microstomus*. To justify synonymization of these two genera, Cooper and Chapleau
521 (1998) have highlighted their autapomorphic character – a continuous cutting edge of uniform teeth in
522 the upper and lower jaws. Unfortunately, phylogenetic relationships among species within the clade with
523 the genus *Microstomus,* including *E. bathybius*, are not fully resolved in our analysis (Fig. 1), and
524 therefore, they must be verified and corrected in future studies.

525 One consequence of synonymyzing *Embassichthys* with *Microstomus* is that we can then argue
526 that *Glyptocephalus* and *Microstomus* should be recognized as sister genera. Previously, Cooper and
527 Chapleau (1998) recognized one autapomorphy for these genera – the intestine extending posteriorly
528 into the body cavity. The phylogenetic relationships of species of *Glyptocephalus* in the present study

529 also support the revision and taxonomic placement of *G. kitaharae* and *G. zachirus* as hypothesized by
530 Cooper and Chapleau (1998). These taxa were previously considered (Sakamoto, 1984) as members of
531 different genera, *Tanakius kitaharae* and *Errex zachirus*. All species of *Glyptocephalus,* including *G.*
532 *kitaharae*, are characterized by a large number (≥ 22) of caudal-fin rays, an apomorphic trait not found
533 among other pleuronectids (Cooper and Chapleau, 1998).

534 *4.3.4. Major monophyletic group IV*

535 The subfamilies Hippoglossinae (excluding genus *Atheresthes*), Lyopsettinae, and Eopsettinae
536 (sensu Nelson et al., 2016) constitute the fourth major monophyletic group on our phylogeny of
537 Pleuronectidae. Its monophyletic hypothesis was previously supported by the following morphological
538 characters (Cooper and Chapleau, 1998): 1) jaw apparatus on ocular and blind sides of the head evenly
539 developed; and 2) multiserial teeth always present on the upper jaws (Norman, 1934). However, our
540 ancestral reconstruction analysis showed that these character states represent plesiomorphies for the
541 family Pleuronectidae.

542 Another notable finding for this clade in the new pleuronectid phylogeny is that two monotypic
543 genera, *Clidoderma* and *Lyopsetta*, are shown as sister taxa. It is noteworthy that *C. asperrimum* and *L.*
544 *exillis* are the only species in the family Pleuronectidae with the disruption in preopercular-mandibular
545 canal of the lateral line system (Voronina, 2005). Although Cooper and Chapleau (1998) did not
546 examine any specimens of *C. asperrimum* in their revision, they placed this species within
547 Hippoglossinae due to its large number of abdominal vertebrae and the presence of a thickened first
548 anal-fin pterygiophore. They have also defined the subfamily Eopsettinae using similar homoplastic
549 characters (Cooper and Chapleau, 1998). Thus, our analysis has shown that the placement of
550 *Clidoderma* within Hippoglossinae can only be accepted if we also add *Lyopsetta* and *Eopsetta* to that
551 subfamily (Fig. 1).

552 *4.3.5. Major monophyletic group V*

553 The fifth major monophyletic group includes all other genera, comprising more than half of all
554 pleuronectid species (Fig. 1). According to present classification of the family Pleuronectidae, this clade
555 includes mainly species from the Pleuronectinae and the Hippoglossoidinae (sensu Nelson et al., 2016).
556 Despite the number of hypothesized synapomorphies proposed in the earlier studies (Cooper and
557 Chapleau, 1998), we did not retrieve monophyletic groups in our phylogeny for either of these taxa.
558 Therefore, the taxonomic nomenclature of both subfamilies should be revised.

559 The subclade, representing all species from the Hippoglossoidinae (sensu Nelson et al., 2016), also
560 included the monotypic *Dexistes* and the polyphyletic *Limanda* in our phylogeny. The latter two genera
561 had previously been related to the Microstomini and the Pleuronectini, respectively (Cooper and
562 Chapleau, 1998; Nelson et al., 2016). Cooper and Chapleau (1998) characterized the subfamily
563 Hippoglossoidinae by the presence of two regular rows of uniform teeth on the fifth ceratobranchial, but
564 they considered this character as homoplastic because it was also found in *Dexistes* and in several other
565 species of the Pleuronectini. However, results of our molecular analysis reveal that this morphological
566 character highlights an important phylogenetic signal for that group.

567 In previous morphological studies (Cooper and Chapleau, 1998; Voronina, 2002), comparison of
568 species from the genus *Limanda* did not provide strong evidence for their monophyly due to a lack of
569 informative apomorphic characters. In her molecular analysis, Roje (2010) found that *L. aspera* and *L.*
570 *sakhalinensis* are sister species, but they do not share the most recent common ancestry with their
571 congeneric species *L. proboscidea*. Our phylogenetic study revealed that the monophyletic group with
572 three species of *Limanda*: *L. aspera*, *L. limanda*, and *L. sakhalinensis*, is placed within the clade also
573 containing Hippoglossoidinae (sensu Nelson et al., 2016). They strongly differ from all other species
574 within this clade by possessing asymmetric jaws, shorter from the blind side, and significantly reduced
575 dentition on the jaws from the ocular side.

576 Three other representatives previously included within *Limanda* (sensu Nelson et al., 2016): *L.*
577 *ferruginea, L. proboscidea*, and *L. punctatissima,* have been hypothesized as a paraphyletic group that is
578 closely related to *Pleuronectes* and *Platichthys* (Fig. 1). Their paraphyly on the BA tree is indicated by
579 the inconsistent phylogenetic position of *L. punctatissima,* which could be an artifact of the long branch
580 attraction (Felsenstein, 2004; Kolaczkowski and Thornton, 2009). However, both *BEAST and
581 ASTRAL species tree analyses placed this species into one monophyletic group with *L. ferruginea* and
582 *L. proboscidea*. Moreover, strong morphological evidence, i.e., in having an extended rugose postorbital
583 ridge (autapomorphic trait), prolonged snout, and the reduction of the supratemporal branch of the
584 lateral line (Norman, 1934; Cooper and Chapleau, 1998; Voronina, 2002), also supports their
585 monophyly. Understanding the phylogenetic importance of these characters, some authors had earlier
586 accepted the subgenus *Myzopsetta* within *Limanda* (Andriashev, 1954; Rass, 1996) or even considered it
587 as the valid genus *Myzopsetta* (Fedorov et al., 2003). The genus name *Myzopsetta* was initially proposed
588 by Gill (1861) for *Platessa ferruginea*, which then had been replaced to *Limanda* by Goode (1881).

589 Thus, we also suggest that *L. ferruginea, L. proboscidea*, and *L. punctatissima* constitute a monophyletic
590 group, whose taxonomic status within the Pleuronectidae should be revised.

591 Polyphyletic structure of *Pleuronectes* was first mentioned by Roje (2010). Our analysis showed
592 that this group is actually paraphyletic, a status that originated with the inclusion of species of *Liopsetta*
593 into *Pleuronectes* (Cooper and Chapleau, 1998). To resolve this situation, we, therefore, think that the
594 genus *Liopsetta*, including three species: *L. glacialis*, *L. pinnifasciatus*, and *L. putnami*, should be
595 accepted as a valid taxon. Monophyly of this genus was also recently supported by several
596 synapomorphic characters, including a shortened infraorbital canal of the lateral line system and the
597 small size of scales (Voronina and Chanet, 2014). Recognition of the monophyly of *Liopsetta*,
598 accordingly affects the status of *Pleuronectes*, which in this restricted sense is characterized by the
599 presence of a series of bony tubercles on the ocular side of the head (autapomorphic state). As restricted,
600 *Pleuronectes* includes only two species: *P. platessa* and *P. quadrituberculatus* (Norman, 1934).

601 Our analysis has also confirmed the conclusions derived from a morphological revision of *P.*
602 *bicoloratus* (Cooper and Chapleau, 1998). Previous to the study by Cooper and Chapleau (1998), this
603 species had been classified in the monotypic *Kareius* because of its highly distinctive autapomorphic
604 character – contiguous bony plates above and below the lateral line (Sakamoto, 1984).

605 *4.4. Questionable species*

606 As in Kartavtsev et al. (2007, 2016), the phylogenetic relationships between *Hippoglossoides*
607 *elassodon* and *H. robustus* were not resolved in our analysis (Fig. 1). However, we found that some
608 monophyletic groups formed by the individuals of these two species correspond to different populations,
609 isolated geographically (Fig. 2). Unresolved relationships were also observed for *Cleisthenes*
610 *herzensteini* and *C. pinetorum*, collected at opposite regions of the Sea of Japan. For both
611 *Hippoglossoides* and *Cleisthenes*, there is a lack of informative morphological characters that could help
612 to distinguish species within each pair mentioned above (Norman, 1934; Sakamoto, 1984; Cooper and
613 Chapleau, 1998). Therefore, we conclude that those species pairs might represent synonymous taxa.

614 Two halibut species from the genus *Hippoglossus* also showed very recent divergence and
615 somewhat unresolved relationships. One of the individuals of *H. hippoglossus* presumably collected in
616 the UK waters was revealed as a sister lineage to its congeneric species *H. stenolepis* from the Pacific
617 Ocean, forming a monophyletic group that is sister to a second individual of *H. hippoglossus* from the
618 southern waters of Sweden (Fig. 1). However, our genetic analysis does not allow us to make any strong

619 inference about the taxonomic status of these two species of halibuts because the first individual of *H.*
620 *hippoglossus* lacks a voucher specimen and all sequences from the second one were obtained from
621 GenBank.

622 In other cases, we found strong molecular evidence to support recognition of both
623 *Pseudopleuronectes schrenki* and *P. yokohamae*, nominal species that were previously considered by
624 several authors as synonymous based on their strong morphological similarity (Norman, 1934; Vinnikov
625 et al., 2006). These two sister species are probably isolated geographically and their population structure
626 should be investigated further with a much larger sample size than we used in the current study.

627 Another important finding of our study confirms the taxonomic validity of *M. shuntovi*, a rare
628 species of the Pleuronectidae collected from the Hawaiian-Emperor seamount chain in the northern
629 Pacific Ocean (Borets, 1983).

630 Additionally, our analysis supports the taxonomic validity of the recently described *Lepidopsetta*
631 *polyxystra* (Orr and Matarese, 2000). For that species, we examined four individuals collected from
632 different locations in the Northern Pacific (Table S2); and all of them have shown very high genetic
633 similarity (Fig. 1). Our study also confirms the vast distribution of *L. polyxystra* in the Northern Pacific,
634 a range that overlaps with those of the other two species from this genus.

635 Our phylogenetic analysis also reveals a potentially new species in the genus *Platichthys* (Fig. 1).
636 This genus currently consists of three extant species, two of which have extremely widespread
637 distributions in comparison with nearly all other pleuronectids. *Platichthys flesus* occurs in the coastal
638 and brackish waters of the Eastern Atlantic, ranging from the White Sea to the Mediterranean and the
639 Black seas (Nielsen, 1986). *Platichthys stellatus,* the starry flounder, is one of the most common
640 nearshore benthic fishes in the Northern Pacific, whose distribution ranges from the Yellow Sea along
641 the coastal zones of Korean Peninsula, Russian Far East, and Japanese archipelago to the Arctic,
642 including the Chukchi and the Beaufort seas, and then extends to the south through the Bering Sea to
643 California (Mecklenburg and Steinke, 2015; Pietsch and Orr, 2015). Conversely, the third species of this
644 genus, *P. bicoloratus*, has a narrow distribution – this species is endemic to the East China Sea and the
645 coastal waters of southern Japan. In our study, we included individuals of *P. stellatus* collected from
646 distant localities of the eastern and western Pacific (Table S1). Possibly, the wide separation between
647 these populations can explain the significant genetic distance we observed between them. It is also
648 noteworthy that samples from the western Pacific were all dextral (right-eyed) variants of that species,

while those fish collected near Japan were all sinistral (left-eyed). Therefore, we think that a large scale population analysis with broad sampling from different regions of the northern Pacific is still needed in order to assess the validity of this taxon and to define the boundaries of its biogeographic distribution. Great attention should be paid to samples from the Bering Sea where two species might interbreed and produce hybrids.

4.5. Taxonomic revision

The current study has revealed the non-monophyly of all subfamilies and tribes described previously for the family Pleuronectidae based on morphological characters (Norman, 1934; Sakamoto, 1984; Cooper and Chapleau, 1998; Evseenko, 2004; Nelson et al., 2016). Here, according to their monophyly, we propose new nomenclature for taxonomic groups that reflect the evolutionary lineages among species of righteye flounders assigned to the Pleuronectidae.

We recognize five major monophyletic groups on the pleuronectid phylogeny that should be classified in the following subfamilies: Atheresthinae, Pleuronichthyinae, Microstominae, Hippoglossinae, and Pleuronectinae. Additionally, the subfamily Pleuronectinae should include two tribes, Hippoglossoidini and Pleuronectini, to denote the corresponding sister monophyletic groups.

Following the principle of monophyly to diagnose lineages of pleuronectid genera, our analysis has confirmed the valid generic status of *Liopsetta* and *Myzopsetta*. It also provided evidence for synonymy of *Embassichthys* and *Microstomus*, for which we recommend using *Microstomus* as the priority name for the genus. The resulting pleuronectid phylogeny has also revealed two species names with questionable taxonomic validity. As in Kartavtsev et al. (2007), we propose that *Hippoglossoides robustus* Gill and Townsend, 1897 is a junior subjective synonym of *Hippoglossoides elassodon* Jordan and Gilbert, 1880a. We also recognize *Cleisthenes pinetorum* Jordan and Starks, 1904 as the senior synonym of *C. herzensteini* (Schmidt, 1904). We prioritized the first species name because it was published on August 13, 1904 (Jordan and Starks, 1904), while the latter name appeared after September 20, 1904, a date declared in the book's preface (Schmidt, 1904). Therefore, the species compositions of *Cleisthenes*, *Hippoglossoides*, *Limanda, Microstomus,* and *Pleuronectes* have been changed corresponding to all corrections in pleuronectid taxonomy described above.

Diagnostic characters for subfamilies, tribes, and for two revised genera, *Limanda* and *Myzopsetta*, were taken from the literature (Norman, 1934; Sakamoto, 1984; Cooper and Chapleau, 1998; Voronina, 2002, 2005) and from personal examination of the museum specimens. Many morphological traits

require further investigation for testing their apomorphic states. The revised classification of the family Pleuronectidae now includes 24 genera and 59 species.

Family PLEURONECTIDAE Rafinesque, 1815

Diagnosis. See the list of morphological synapomorphies in Cooper and Chapleau (1998). Their statements need further examination with a larger number of outgroup taxa.

Subfamily Atheresthinae subfam. nov.

Type genus. *Atheresthes* Jordan and Gilbert, 1880b: 51 (feminine; type species *Platysomatichthys stomias* Jordan and Gilbert, 1880b by original designation and monotypy; holotype: ?USNM 27186 (1 of 3)). Diagnosis. Synapomorphies: 1) distinct curvature along the ventral margin of metapterygoid; 2) barbed teeth with two enlarged canine-like teeth in front; 3) opening between the dorsal and ventral hypohyals of a hyoid arch. Posteriormost abdominal vertebra has haemapophysis formed by the fusion of parapophyses. The last neural spine is connected with the only unsegmented ray in the caudal fin. Parhypural is ventrally adjacent to the plate formed by the first and second hypurals. Symmetrical maxillae are longer than half of the head length and extend to beyond the eyes. Barbed biserial teeth equally developed on both jaws and on the pharyngeal arch. Long and slender gill rakers with small spurs at the tip are present on both parts of a gill arch. Caudal fin is lunate-shaped. A distinct curvature of the lateral line above the pectoral fins is absent. Olfactory lamellae arranged radially around a central rachis. Scales are present on eyes and on all fins. 12 abdominal and 37–39(41) caudal vertebrae. Genus *Atheresthes* Jordan and Gilbert, 1880b with two species: *A. evermanni*, *A. stomias*.

Subfamily Pleuronichthyinae subfam. nov.

Type genus. *Pleuronichthys* Girard, 1854: 139 (masculine; type species *Pleuronichthys coenosus* Girard, 1854 by monotypy; syntypes: USNM 697). Diagnosis. Synapomorphies: 1) reduced number of caudal vertebrae (22–25); 2) multiple rows of small slender villiform teeth always present on premaxillary and dentary from the blind side; 3) thick lips with transverse plicae on the inner side (plicae is not reported for *P. guttulatus*); 4) accessory branch in the supratemporal canal of the lateral line extending along the dorsal fin to the posterior part of the body; 5) large foramen in prefrontal from the blind side; 6) lateral process on frontal from the ocular side; 7) both pterosphenoids strongly reduced; 8) 0–2 gill rakers on second hypobranchial; 9) absence of dentition on the ventral surface of third epibranchial. Except for *P. guttulatus*: 1) eyes separated by a high interorbital ridge with strong bony spines or protuberances; 2) dorsal fin originates on the blind side of the head; 3) reduced or absent cartilaginous interspace between

parasphenoid and prefrontal from the blind side; 4) mesethmoid forming only the anterior margin of the upper orbit; 5) teeth usually completely absent on premaxillary and dentary from the ocular side. All scales are cycloid. 12–14(15) abdominal and 22–25(26) caudal vertebrae.

Genus *Pleuronichthys* Girard, 1854 with eight species: *P. coenosus*, *P. cornutus*, *P. decurrens*, *P. guttulatus*, *P. lighti*, *P. ocellatus*, *P. ritteri*, *P. verticalis*.

Subfamily Microstominae subfam. nov.

Type genus. *Microstomus* Gottsche, 1835: 136, 150 (masculine; type species *Microstomus latidens* Gottsche, 1835 by monotypy; whereabouts unknown). Diagnosis. Synapomorphies: 1) elongated second loop of intestine, extending into the posterior body cavity from the ocular side; 2) less than five infraorbital bones; 3) incisorlike teeth forming a continuous cutting edge; 4) single row of teeth on premaxillary and dentary. Hyomandibular is without a broad anteroventral margin (reversal). 11–14 abdominal and 35–51 caudal vertebrae.

Genus *Glyptocephalus* Gottsche, 1835 with four species: *G. cynoglossus*, *G. kitaharae*, *G. stelleri*, *G. zachirus*.

Genus *Microstomus* Gottsche, 1835 with five species: *M. achne*, *M. bathybius*, *M. kitt*, *M. pacificus*, *M. shuntovi*.

Subfamily Hippoglossinae Gill, 1864

Type genus. *Hippoglossus* Cuvier, 1816: 221 (masculine; type species *Pleuronectes hippoglossus* Linnaeus, 1758 by absolute tautonymy; syntypes: BMNH 1853.11.12.127). Diagnosis. Currently no synapomorphic characters have been recognized in adults. Roje (2010) mentioned scattered melanophores in the median finfolds of flexion larvae. All other shared morphological characters are considered as symplesiomorphies. Bony plates are present on the branchial arch. Nearly symmetrical maxillaries are at least 1/2 of the head length and extend to or behind a pupil of the eyes. Teeth of different shapes and size are well-developed from both sides and always have multiple rows on premaxillae. Except for *C. asperrimum*, dentition is present on the ventral surface of third epibranchial. 11–19 abdominal and 27–45 caudal vertebrae.

Genus *Clidoderma* Bleeker, 1862 with one species: *C. asperrimum.*

Genus *Eopsetta* Jordan and Goss in Jordan, 1885 with two species: *E. grigorjewi*, *E. jordani*.

Genus *Hippoglossus* Cuvier, 1816 with two species: *H. hippoglossus*, *H. stenolepis*.

Genus *Lyopsetta* Jordan and Goss in Jordan, 1885 with one species: *L. exilis.*

Genus *Reinhardtius* Gill, 1861 with one species: *R. hippoglossoides.*

Genus *Verasper* Jordan and Gilbert in Jordan and Evermann, 1898 with two species: *V. moseri*, *V. variegatus*.

Subfamily Pleuronectinae Rafinesque, 1815

Type genus. *Pleuronectes* Linnaeus, 1758: 268 (masculine; type species *Pleuronectes platessa* Linnaeus, 1758 by subsequent designation; syntypes: BMNH 1853.11.12.130–131). Diagnosis. Synapomorphies: 1) complete reduction of interorbital process; 2) hyomandibular with a broad anteroventral margin; 3) absence of dentition on ventral surface of third epibranchial; 4) premaxillary and dentary teeth always uniserial. Except for *Isopsetta*, haemal spine in anteriormost caudal vertebra is narrow in base without lateral foramen in haemal arch. Except for *Isopsetta, Lepidopsetta* and *Psettichthys*, multiple rows of teeth are present on fifth ceratobranchial. 9–13 abdominal and 24–34 caudal vertebrae.

Tribe Hippoglossoidini Cooper and Chapleau, 1998

Type genus. *Hippoglossoides* Gottsche, 1835: 164, 168 (masculine; type species *Hippoglossoides limanda* Gottsche, 1835 (= *Pleuronectes limandoides* Bloch, 1787) by monotypy; lectotype: whereabouts unknown). Diagnosis. Currently no synapomorphic characters have been recognized. Maxillaries always extend to beyond the anterior margin of the lower eye. Conical teeth on premaxillary and dentary are in a single irregular row and do not make a uniform cutting edge. Except for *Limanda*, maxillaries are symmetric or nearly symmetric, and fifth ceratobranchial bears two regular rows of teeth. Except for *A. nadeshnyi*, supraorbital canal of the lateral line system is absent on the blind side. 9–13 abdominal and 29–34 caudal vertebrae.

Genus *Acanthopsetta* Schmidt, 1904 with one species: *A. nadeshnyi*.

Genus *Cleisthenes* Jordan and Starks, 1904 with one species: *C. pinetorum*.

Genus *Dexistes* Jordan and Starks, 1904 with one species: *D. rikuzenius*.

Genus *Hippoglossoides* Gottsche, 1835 with three species: *H. dubius*, *H. elassodon*, *H. platessoides*.

Genus *Limanda* Gottsche, 1835 (feminine; type species *Limanda vulgaris* Gottsche, 1835 (= *Pleuronectes limanda* Nillson [= Linnaeus, 1758]) by monotypy; no types known) with three species: *L. aspera*, *L. limanda*, *L. sakhalinensis*. Diagnosis. Currently no synapomorphic characters have been recognized. Distinct rugose postorbital ridge is absent. Scales are partially embedded and imbricated having numerous ctenii from the ocular side. Maxillaries are asymmetric, shorter from the blind side. Number of teeth from the ocular side is usually greater than 6 but almost twice less than on the blind side. Distal end of the first epibranchial is bifurcated. Supratemporal canal of the lateral line is well-developed. 9–11 abdominal and 29–31 caudal vertebrae.

Tribe Pleuronectini Nelson, 1984

Type genus. Pleuronectes Linnaeus, 1758: 268 (masculine; type species *Pleuronectes platessa* Linnaeus, 1758 by subsequent designation; syntypes: BMNH 1853.11.12.130–131). Diagnosis. Synapomorphies: 1) short and strongly asymmetric maxillaries not reaching the pupil of the lower eye; 2) distal end of the first epibranchial without bifurcation; 3) obtusely conical or incisorlike teeth on premaxillary and dentary usually make a uniform cutting edge. Maxillaries are asymmetric, shorter from the blind side. 10–13 abdominal and 24–34 caudal vertebrae.

Genus *Isopsetta* Lockington, 1880 with one species: *I. isolepis*.

Genus *Lepidopsetta* Gill, 1862 with three species: *L. bilineata*, *L. mochigarei*, *L. polyxystra*.

Genus *Liopsetta* Gill, 1864 with three species: *L. glacialis*, *L. pinnifasciata*, *L. putnami*.

Genus *Myzopsetta* Gill, 1861 (feminine; type species *Platessa ferruginea* Storer 1839 by subsequent designation; holotype: whereabouts unknown) with three species: *M. ferruginea*, *M. proboscidea*, *M. punctatissima*. Diagnosis. Synapomorphies: 1) supratemporal canal of the lateral line strongly reduced having 3–6 pores from the ocular side and 2–3 pores from the blind side; 2) upper profile of the head distinctly concaved above the upper eye, protruding a snout; 3) maxillaries scarcely reach the anterior margin of the lower eye; 4) broad and strongly rugose postorbital ridge; 5) blind side has yellow stripes or complete yellow coloration. More than 10 conical teeth always present on premaxillary and dentary from the ocular side. Dorsal margin of prootic foramen is formed by sphenotic. 10–12 abdominal and 25–33 caudal vertebrae.

Genus *Parophrys* Girard, 1854 with one species: *P. vetulus*.

Genus *Platichthys* Girard, 1854 with three species: *P. bicoloratus*, *P. flesus*, *P. stellatus*.

Genus *Pleuronectes* Linnaeus, 1758 with two species: *P. platessa*, *P. quadrituberculatus*.

Genus *Pseudopleuronectes* Linnaeus, 1758 with five species: *P. americanus*, *P. herzensteini*, *P. obscurus*, *P. schrenki*, *P. yokohamae*.

Genus *Psettichthys* Girard, 1854 with one species: *P. melanostictus*.

5. Conclusions

Our study has resulted in a well resolved phylogeny of the family Pleuronectidae and has provided strong molecular evidence for its taxonomic revision and reassessment of morphological diagnostic characters. We have revealed homoplasy among several character states previously considered as synapomorphies in the systematics of pleuronectid species. Such patterns of convergent evolution might be due to morphological responses to similar ecological conditions experienced by different species of flounders that do not share a common ancestry. Indeed, representatives of various pleuronectid genera very often co-occur together in the same benthic habitats, and therefore, could have independently developed similar adaptive characteristics.

The resulting phylogeny also contained several nodes with poor statistical support. The hypothesized relationships for these lineages will need to be confirmed in future studies. These nodes represent the relationships among species within the subfamilies Microstominae and Hippoglossinae, the new classification that we proposed in the current study. Our analysis also supports the questionable validity of both *Cleisthenes herzensteini* and *Hippoglossoides robustus*. Therefore, we suggest the first species as the junior subjective synonym of *C. pinetorum*, whose distributional range is restricted to the Sea of Japan and the East China Sea. We also hypothesize that *Hippoglossoides robustus* is not a valid species, but represents the arctic populations of its senior synonym – *H. elassodon*. We also recommend that all taxa within *Cleisthenes*, *Hippoglossoides*, and *Platichthys* be analyzed using much larger sample sizes than were incorporated in the current study in order to establish the intraspecific limits of morphological variation among these taxa, especially to determine geographical differences among their populations, and then compare these results to results presented in the current study.

Acknowledgments

Funding for this project, including all experimental work, was provided to KV by the Russian Science Foundation, grant number 14-50-00034. We sincerely thank Ted Pietsch and Katherine Maslennikov, Burke Museum of the University of Washington, USA (UW); Ed Wiley and Andrew Bentley, the University of Kansas Biodiversity Institute and Natural History Museum, USA (KU); H.J. Walker, Scripps Institution of Oceanography, University of California at San Diego, USA (SIO); Takeshi Tomiyama, Hiroshima University, Japan (HUM); Koichi Hoshino, Seikai National Fisheries Research Institute, Japan (SNFR); Yoshiaki Kai, Kyoto University, Japan (FAKU); Elena Voronina, Zoological Institute of the Russian Academy of Sciences, Russia (ZIN); Dmitry Lajus, Saint-Petersburg University, Russia; Andrey Balanov and Sergei Turanov, Institute of Marine Biology of the Far Eastern Branch of the Russian Academy of Sciences, Russia (MIMB); Irina Volvenko, Zoological Museum of the Far Eastern Federal University, Russia (ZMFESU); and Noel Alfonso, Canadian Museum of Nature, Canada (CMN) for lending voucher specimens and tissue samples. Special thanks to Sandra Raredon, Smithsonian Institution National Museum of Natural History, for doing X-ray imaging of the museum specimens. We sincerely acknowledge Lynne Parenti, Smithsonian Institution National Museum of Natural History; Kathleen Cole, Helena Barreto and Jessica Maxfield, University of Hawaii at Manoa, for reading this manuscript and providing valuable feedback. We are also very grateful to the editor and all three reviewers of the manuscript for their excellent comments and recommendations.

837 **References**

838 Akaike, H., 1973. Information theory and an extension of the maximum likelihood principle, in:
839 Petrov, B.N., Csaki, F. (Eds.), Second International Symposium on Information Theory.
840 Akademiai Kiado, Budapest, pp. 267–281.
841 Andriashev, A.P., 1954. Fishes of the northern seas of the USSR. Akad. Nauk SSSR, Moscow
842 and Saint-Petersburg.
843 Benson, D.A., Cavanaugh, M., Clark, K., Karsch-Mizrachi, I., Lipman, D.J., Ostell, J., Sayers,
844 E.W., 2017. GenBank. Nucleic Acids Res. 45, D37–D42.
845 Berendzen, P.B., Dimmick, W.W., 2002. Phylogenetic relationships of Pleuronectiformes based
846 on molecular evidence. Copeia, 642–652.
847 Betancur-R, R., Li, C., Munroe, T.A., Ballesteros, J.A., Ortí, G., 2013a. Addressing gene tree
848 discordance and non-stationarity to resolve a multi-locus phylogeny of the flatfishes
849 (Teleostei: Pleuronectiformes). Syst. Biol. 62, 763–785.
850 Betancur-R, R., Broughton, R.E., Wiley, E.O., Carpenter, K., López, J.A., Li, C., Holcroft, N.I.,
851 Arcila, D., Sanciangco, M., Cureton Ii, J.C., Zhang, F., 2013b. The tree of life and a new
852 classification of bony fishes. PLOS Currents Tree of Life.
853 Betancur-R, R., Wiley, E.O., Arratia, G., Acero, A., Bailly, N., Miya, M., Lecointre, G., Ortí, G.,
854 2017. Phylogenetic classification of bony fishes. BMC Evol. Biol. 17, 162.
855 Bleeker, P., 1862. Sur quelques genres de la famille des Pleuronectoïdes. Versl. Akad.
856 Amsterdam 13, 422–429.
857 Bloch, M.E., 1787. Naturgeschichte der ausländischen Fische. Vol. 3. Morino, Berlin.
858 Borets, L.A., 1983. A new species of flounder, *Microstomus shuntovi* sp. n. (Pleuronectidae), and
859 two rare flounder species (Bothidae) from seamounts of the northwestern and Hawaiian
860 Ridges. J. Ichthyol. 23, 1–6.
861 Bouckaert, R., Heled, J., Kühnert, D., Vaughan, T., Wu, C.H., Xie, D., Suchard, M.A., Rambaut,
862 A., Drummond, A.J., 2014. BEAST 2: a software platform for Bayesian evolutionary
863 analysis. PLoS Comput. Biol. 10, e1003537.
864 Bouckaert, R.R., 2010. DensiTree: making sense of sets of phylogenetic trees. Bioinformatics
865 26, 1372–1373.
866 Campbell, M.A., Chen, W.J., López, J.A., 2013. Are flatfishes (Pleuronectiformes)
867 monophyletic? Mol. Phylogenet. Evol. 69, 664–673.

868 Campbell, M.A., López, J.A., Satoh, T.P., Chen, W.J., Miya, M., 2014. Mitochondrial genomic
869 investigation of flatfish monophyly. Gene 551, 176–182.
870 Chapleau, F., Keast, A., 1988. A phylogenetic reassessment of the monophyletic status of the
871 family Soleidae, with comments on the suborder Soleoidei (Pisces; Pleuronectiformes).
872 Can. J. Zool. 66, 2797–2810.
873 Cooper, J.A., Chapleau, F., 1998. Monophyly and interrelationships of the family Pleuronectidae
874 (Pleuronectiformes), with a revised classification. Fish. Bull. 96, 686–726.
875 Cracraft, J., 1983. Species concepts and speciation analysis, in Johnston, R.F. (Ed.), Current
876 ornithology. New York: Plenum Press, pp. 159–187.
877 Cuvier, G., 1816. Le règne animal distribué d'après son organisation pour servir de base à
878 l'histoire naturelle des animaux et d'introduction à l'anatomie comparée. Les reptiles, les
879 poissons, les mollusques et les annélides. Deterville, Paris.
880 Darriba, D., Taboada, G.L., Doallo, R., Posada, D., 2012. jModelTest 2: more models, new
881 heuristics and parallel computing. Nat. Methods 9, 772–772.
882 de Queiroz, K., 1998. The general lineage concept of species, species criteria, and the process of
883 speciation: A conceptual unification and terminological recommendations, in: Howard,
884 D.J., Berlocher, S.H. (Eds.). Endless forms: species and speciation. Oxford University
885 Press, New York, pp. 57–75.
886 Drummond, A.J., Ho, S.Y., Phillips, M.J., Rambaut, A., 2006. Relaxed phylogenetics and dating
887 with confidence. PLoS Biol. 4, e88.
888 Edgar, R.C., 2004. MUSCLE: multiple sequence alignment with high accuracy and high
889 throughput. Nucleic Acids Res. 32, 1792–1797.
890 Evseenko, S.A., 2004. Family Pleuronectidae Cuvier 1816 – righteye flounders. Calif. Acad. Sci.
891 Annot. Checkl. Fish. 37.
892 Fan, Y., Wu, R., Chen, M.H., Kuo, L., Lewis, P.O., 2011. Choosing among partition models in
893 Bayesian phylogenetics. Mol. Biol. Evol. 28, 523–532.
894 Fedorov, V.V., Chereshnev, I.A., Nazarkin, M.V., Shestakov A.V., Volobuev V.V., 2003.
895 Catalog of marine and freshwater fishes of the northern part of the Sea of Okhotsk.
896 Dalnauka, Vladivostok.
897 Felsenstein, J., 1985. Phylogenies and the comparative method. Am. Nat. 125, 1–15.
898 Felsenstein, J. 2004. Inferring Phylogenies. Sinauer Associates, Sunderland.

899 Fitch, J.E., 1963. A review of the fishes of the genus *Pleuronichthys*. Los. Anngel. County Mus.
900 Contrib. Sci. 76, 3–33.
901 Gill, T.N., 1861. Catalogue of the fishes of the eastern coast of North America, from Greenland
902 to Georgia. Proc. Acad. Nat. Sci. Philadelphia 13, 1–63.
903 Gill, T.N., 1862. Note on some genera of fishes of western North America. Proc. Acad. Nat. Sci.
904 Philadelphia 14: 329–332.
905 Gill, T.N., 1864. Synopsis of the pleuronectoids of California and north-western America. Proc.
906 Acad. Nat. Sci. Philadelphia 16, 194–198.
907 Gill, T.N., Townsend, C.H., 1897. Diagnoses of new species of fishes found in Bering Sea. Proc.
908 Biol. Soc. Wash. 11, 231–234.
909 Girard, C.F., 1854. Descriptions of new fishes, collected by Dr. A. L. Heermann, naturalist
910 attached to the survey of the Pacific railroad route, under Lieut. R. S. Williamson, U.S.A.
911 Proc. Acad. Nat. Sci. Philadelphia 7: 129–140.
912 Goode, G.B., 1881. Fishes from the deep water on the south coast of New England obtained by
913 the United States Fish Commission in the summer 1880. Proc. U.S. Nat. Mus. 3, 467–
914 486.
915 Gottsche, C.M., 1835. Die seeländischen Pleuronectes-Arten. Archiv für Naturgeschichte 2:
916 133–185.
917 Harrington, R.C., Faircloth, B.C., Eytan, R.I., Smith, W.L., Near, T.J., Alfaro, M.E., Friedman,
918 M., 2016. Phylogenomic analysis of carangimorph fishes reveals flatfish asymmetry
919 arose in a blink of the evolutionary eye. BMC Evol. Biol. 16, 224.
920 Heled, J., Drummond, A.J., 2010. Bayesian inference of species trees from multilocus data. Mol.
921 Biol. Evol. 27, 570–580.
922 Jermiin, L.S., Ho, S.Y., Ababneh, F., Robinson, J., Larkum, A.W., 2004. The biasing effect of
923 compositional heterogeneity on phylogenetic estimates may be underestimated. Syst.
924 Biol. 53, 638–643.
925 Ji, H.S., Kim, J.K., Kim, B.J., 2016. Molecular phylogeny of the families Pleuronectidae and
926 Poecilopsettidae (PISCES, Pleuronectiformes) from Korea, with a proposal for a new
927 classification. Ocean Sci. J. 51, 299–304.

928 Jordan, D.S., 1885. A catalogue of the fishes known to inhabit the waters of North America,
929 north of the Tropic of Cancer, with notes on species discovered in 1883 and 1884. U.S.
930 Comm. Fish and Fisheries 13, 789–973.
931 Jordan, D.S., Evermann, B.W., 1898. The fishes of North and Middle America: a descriptive
932 catalogue of the species of fish-like vertebrates found in the waters of North America,
933 north of the Isthmus of Panama. Part III. Bull. U.S. Nat. Mus. 47, 2183–3136.
934 Jordan, D.S., Gilbert, C.H., 1880a. Description of two new species of flounders (*Parophrys*
935 *ischyrus* and *Hippoglossoides elassodon*), from Puget's Sound. Proc. U.S. Nat. Mus. 147,
936 276–279.
937 Jordan, D.S., Gilbert, C.H., 1880b. Description of a new flounder (*Platysomatichthys stomias*),
938 from the coast of California. Proc. U.S. Nat. Mus. 152, 301–303.
939 Jordan, D. S., Goss, D.K., 1889. A review of the flounder and soles Pleuronectidae of America
940 and Europe. Rep. U.S. Com. Fish. Washington 14, 225–342.
941 Jordan, D.S., Starks E.C., 1904. List of fishes dredged by the steamer Albatross off the coast of
942 Japan in the summer of 1900, with descriptions of new species and a review of the
943 Japanese Macrouridae. Bull. U.S. Fish Comm. 22, 577–630.
944 Kartavtsev, Y.P., Park, T.J., Vinnikov, K.A., Ivankov, V.N., Sharina, S.N., Lee, J.S., 2007.
945 Cytochrome b (Cyt-b) gene sequence analysis in six flatfish species (Teleostei,
946 Pleuronectidae), with phylogenetic and taxonomic insights. Mar. Biol. 152, 757–773.
947 Kartavtsev, Y.P., Sharina, S.N., Saitoh, K., Imoto, J.M., Hanzawa, N., Redin, A.D., 2016.
948 Phylogenetic relationships of Russian far eastern flatfish (Pleuronectiformes,
949 Pleuronectidae) based on two mitochondrial gene sequences, Co-1 and Cyt-b, with
950 inferences in order phylogeny using complete mitogenome data. Mitochondr. DNA 27,
951 667–678.
952 Kass, R.E., Raftery, A.E., 1995. Bayes factors. J. Am. Stat. Assoc. 90, 773–795.
953 Kearse, M., Moir, R., Wilson, A., Stones-Havas, S., Cheung, M., Sturrock, S., Buxton, S.,
954 Cooper, A., Markowitz, S., Duran, C., Thierer, T., 2012. Geneious Basic: an integrated
955 and extendable desktop software platform for the organization and analysis of sequence
956 data. Bioinformatics 28, 1647–1649.
957 Kolaczkowski, B., Thornton, J.W., 2009. Long-branch attraction bias and inconsistency in
958 Bayesian phylogenetics. PLoS One 4, e7891.

959 Kumar, S., Gadagkar, S.R., 2001. Disparity index: a simple statistic to measure and test the
960 homogeneity of substitution patterns between molecular sequences. Genetics 158, 1321–
961 1327.
962 Kumar, S., Stecher, G., Tamura, K., 2016. MEGA7: Molecular Evolutionary Genetics Analysis
963 version 7.0 for bigger datasets. Mol. Biol. Evol. 33, 1870–1874.
964 Lanfear, R., Calcott, B., Ho, S.Y., Guindon, S., 2012. PartitionFinder: combined selection of
965 partitioning schemes and substitution models for phylogenetic analyses. Mol. Biol. Evol.
966 29, 1695–1701.
967 Lockington W.N., 1880. Note on a new flatfish (*Lepidopsetta isolepis*) found in the markets of
968 San Francisco. Proc. U.S. Nat. Mus. 158, 325.
969 Linnaeus, C. 1758. Systema naturae per regna tria naturae, secundum classes, ordines, genera,
970 species, cum characteribus, differentiis, synonymis, locis. Tomus I. Editio decima,
971 reformata. Laurentius Salvius, Stockholm.
972 Mecklenburg, C.W., Steinke, D., 2015. Ichthyofaunal baselines in the Pacific Arctic region and
973 RUSALCA study area. Oceanography 28, 158–189.
974 Miller, M.A., Schwartz, T., Pickett, B.E., He, S., Klem, E.B., Scheuermann, R.H., Passarotti, M.,
975 Kaufman, S., O'Leary, M.A., 2015. A RESTful API for access to phylogenetic tools via
976 the CIPRES science gateway. Evol. Bioinformatics 11, 43–48.
977 Mirarab, S., Warnow, T., 2015. ASTRAL-II: coalescent-based species tree estimation with many
978 hundreds of taxa and thousands of genes. Bioinformatics 31, i44–i52.
979 Near, T.J., Eytan, R.I., Dornburg, A., Kuhn, K.L., Moore, J.A., Davis, M.P., Wainwright, P.C.,
980 Friedman, M., Smith, W.L., 2012. Resolution of ray-finned fish phylogeny and timing of
981 diversification. Proc. Natl. Acad. Sci. USA, 109, 13698–13703.
982 Nelson, J.S., 1984. Fishes of the world, 2nd ed. John Wiley and Sons, New York.
983 Nelson, J.S., Grande, T.C., Wilson, M.V., 2016. Fishes of the world, 5th ed. John Wiley and
984 Sons, Hoboken.
985 Nielsen, J.G., 1986. Pleuronectidae, in: Whitehead, P.J.P., Bauchot, M.L., Hureau, J.C., Nielsen,
986 J., Tortonese, E. (Eds.). Fishes of the eastern Atlantic and the Mediterranean. UNESCO,
987 Paris, pp. 1299–1307.
988 Norman, J.R., 1934. A systematic monograph of the flatfishes (Heterosomata). British Museum
989 of Natural History, London.

990 Orr, J.W., Matarese, A.C., 2000. Revision of the genus *Lepidopsetta* Gill, 1862 (Teleostei:
991 Pleuronectidae) based on larval and adult morphology, with a description of a new
992 species from the North Pacific Ocean and Bering Sea. Fish. Bull. 98, 539–539.
993 Paradis, E., Claude, J., Strimmer, K., 2004. APE: analyses of phylogenetics and evolution in R
994 language. Bioinformatics 20, 289–290.
995 Penny, D., Hendy, M.D., 1985. The use of tree comparison metrics. Syst. Zool. 34, 75–82.
996 Pietsch, T.W., Orr, J.W., 2015. Fishes of the Salish Sea: a compilation and distributional
997 analysis. NOAA Professional Paper NMFS 18. NOAA, Seattle.
998 R Core Team, 2016. R: a language and environment for statistical computing. R foundation for
999 statistical computing, Vienna. https://www.R-project.org/
1000 Rafinesque, C.S., 1815. Analyse de la nature, ou tableau de l'univers et des corps organises. Jean
1001 Barravecchia, Palerme.
1002 Rambaut, A., Suchard, M.A., Xie, D., Drummond, A.J., 2014. Tracer v1.6.1.
1003 http://tree.bio.ed.ac.uk/software/tracer/
1004 Rass, T.S., 1996. On taxonomy of Pleuronectini (Pleuronectidae). J. Ichthyol. 36, 546–548.
1005 Revell, L.J., 2012. phytools: an R package for phylogenetic comparative biology (and other
1006 things). Methods Ecol. Evol. 3, 217–223.
1007 Richards, E.J., Brown, J.M., Barley, A.J., Chong, R.A., Thomson, R.C., 2018. Variation across
1008 mitochondrial gene trees provides evidence for systematic error: How much gene tree
1009 variation is biological? Syst. Biol. Advance online publication. doi:
1010 10.1093/sysbio/syy013
1011 Roje, D.M., 2010. Incorporating molecular phylogenetics with larval morphology while
1012 mitigating the effects of substitution saturation on phylogeny estimation: A new
1013 hypothesis of relationships for the flatfish family Pleuronectidae (Percomorpha:
1014 Pleuronectiformes). Mol. Phylogenet. Evol. 56, 586–600.
1015 Ronquist, F., Teslenko, M., Van Der Mark, P., Ayres, D.L., Darling, A., Höhna, S., Larget, B.,
1016 Liu, L., Suchard, M.A., Huelsenbeck, J.P., 2012. MrBayes 3.2: efficient Bayesian
1017 phylogenetic inference and model choice across a large model space. Syst. Biol. 61, 539–
1018 542.
1019 Sakamoto, K., 1984. Interrelationships of the family Pleuronectidae (Pisces: Pleuronectiformers).
1020 Mem. Fac. Fish. Hokkaido Univ. 31, 95–215.

1021 Schmidt, P.Y., 1904. Fishes of the eastern seas of the Russian Empire. Stasyulevich publishing,
1022 St. Petersburg.
1023 Schwarz, G., 1978. Estimating the dimension of a model. Ann. Stat. 6, 461–464.
1024 Stamatakis, A., 2014. RAxML version 8: a tool for phylogenetic analysis and post-analysis of
1025 large phylogenies. Bioinformatics 30, 1312–1313.
1026 Storer, D.H., 1839. A report on the fishes of Massachusetts. Boston J. Nat. Hist. 2, 289–558.
1027 Suzuki, N., Nishida, M., Amaoka, K., 2001. The phylogenetic position of the genus *Atheresthes*
1028 (Pleuronectidae) and its classification: a molecular phylogenetic approach using
1029 mitochondrial sequence data. Bull. Fish. Sci. Hokkaido Univ. 52, 36–46.
1030 Swofford, D. L. 2002. PAUP*. Phylogenetic analysis using parsimony (*and other methods).
1031 Version 4.0a152. Sinauer Associates, Sunderland.
1032 Untergasser, A., Cutcutache, I., Koressaar, T., Ye, J., Faircloth, B.C., Remm, M., Rozen, S.G.,
1033 2012. Primer3 – new capabilities and interfaces. Nucleic Acids Res. 40, e115–e115.
1034 Vaidya, G., Lohman, D.J., Meier, R., 2011. SequenceMatrix: concatenation software for the fast
1035 assembly of multi-gene datasets with character set and codon information. Cladistics 27,
1036 171–180.
1037 Vinnikov., K.A., Ivankov, V.N., Pitruk, D.L., 2006. Taxonomic status of *Pseudopleuronectes*
1038 *yokohamae* and *P. schrenki* (Pleuronectidae sensu Cooper and Chapleau, 1998). J.
1039 Ichthyol. 46, 301–310.
1040 Voronina, E.P., 2002. Morphology of the acoustico-lateralis system of some pleuronectids:
1041 Communication 1. J. Ichthyol. 42, 555–564.
1042 Voronina, E.P., 2005. Characteristics of the seismosensory system morphology in some
1043 Pleuronectidae. J. Ichthyol. 45, 146–156.
1044 Voronina, E.P., Chanet, B., 2014. Monophyly of the genus *Liopsetta* (Pleuronectidae). Cybium
1045 38, 43–52.
1046 Wilks, S.S., 1938. The large-sample distribution of the likelihood ratio for testing composite
1047 hypotheses. Ann. Math. Stat. 9, 60–62.
1048 Xie, W., Lewis, P.O., Fan, Y., Kuo, L., Chen, M.H., 2011. Improving marginal likelihood
1049 estimation for Bayesian phylogenetic model selection. Syst. Biol. 60, 150–160.

1050 Yokogawa, K., Ogihara, G., Watanabe, K., 2014. Identity of the lectotype of the East Asian
1051 flatfish *Pleuronichthys cornutus* (Temminck and Schlegel 1846) and reinstatement of
1052 *Pleuronichthys lighti* Wu 1929. Ichthyol. Res. 61, 385–392.

Table 1

Nuclear and mitochondrial DNA fragments sequenced in the current study. Compositional base variation for each dataset was assessed by the average GC content (*GC*), chi-square test of homogeneity of state frequencies (χ^2) and the averaged disparity index (I_D). Phylogenetic informativeness of each dataset was estimated from the corresponding maximum likelihood tree. The bootstrap support values were averaged across all internal nodes. PH85 is the topological distance (Penny and Hendy, 1985) between each gene tree and the tree reconstructed from the concatenated dataset.

Locus	Source	Size (bp)	Variable sites (%)	Base heterogeneity			Phylogenetic signal	
				GC	χ^{2} *	I_D	Bootstrap	PH85
COI	DNA_{mt}	1548	672 (43.41)	0.462	139.29**	0.109	84.47	42
cytb	DNA_{mt}	1141	529 (53.64)	0.468	156.59**	0.132	85.47	38
tRNA-Thr	DNA_{mt}	79	29 (36.71)	0.515	51.65**	0.045	12.21	258
RAG1	DNA_{nu}	798	230 (28.82)	0.562	39.41**	0.035	67.18	160
RAG2	DNA_{nu}	861	337 (39.14)	0.579	99.56**	0.118	71.10	134
Rho	DNA_{nu}	1062	420 (39.55)	0.505	26.55**	0.008	73.48	86
Rho-UTR	DNA_{nu}	254	123 (48.43)	0.386	23.63**	0.003	45.87	199

* This chi-square test ignores correlation of base frequencies caused by to phylogenetic signal.

** p-value = 1.00, meaning no indication of base compositional heterogeneity.

Table 2

Comparative analysis of the different partitioning schemes for the concatenated sequence dataset. Bayes factors (log BF) indicate strength of the difference with the best fitted model (shown in bold).

Partitioning scheme	Criterion	N	Partitions	log L	log SS	log BF
1. Genes & Codons	BIC	17	*COI_1, COI_2, COI_3, cytb_1, cytb_2, cytb_3, RAG1_1, RAG1_2, RAG1_3, RAG2_1, RAG2_2, RAG2_3, Rho_1, Rho_2, Rho_3, Rho-UTR, tRNA-Thr*	-57041.17	-57133.15	-601.78
2. **PartitionFinder #1**	AIC	14	*COI_1, COI_2+cytb_2, COI_3, cytb_1, cytb_3, RAG1_1, RAG1_2, RAG1_3+RAG2_3, RAG2_1+RAG2_2, Rho_1, Rho_2, Rho_3, Rho-UTR, tRNA-Thr*	-57221.76	-56531.37	0
3. PartitionFinder #2	BIC	10	*COI_1, COI_2+cytb_2, COI_3, cytb_1+tRNA-Thr, cytb_3, RAG1_1+RAG2_2, RAG1_2+Rho_2, RAG1_3+RAG2_3+Rho_3, RAG2_1+ Rho-UTR, Rho_1*	-57331.33	-56822.89	-291.52
4. Genes	BIC	7	*COI, cytb, RAG1, RAG2, Rho, Rho-UTR, tRNA-Thr*	-58557.72	-58515.95	-1984.58
5. DNA type	BIC	2	*COI+cytb+tRNA-Thr, RAG1+RAG2+Rho+ Rho-UTR*	-58781.21	-58580.58	-2049.21
6. Total evidence	BIC	1	*COI+cytb+RAG1+RAG2+Rho+ Rho-UTR +tRNA-Thr*	-59112.88	-60028.99	-3497.62

N – number of partitions within each scheme; log L – log-likelihood score for the best ML tree reconstructed in RAxML analysis; log SS – sum of the marginal log-likelihoods estimated by Stepping Stone analysis in MrBayes; BF – Bayes factor computed as $log\ BF = log\ SS_{best} - log\ SS_i$, where *i* is the partitioning scheme. The numbers after underscores in partition names indicate different codon positions within a protein coding sequence.

Figure captions

Fig. 1. Bayesian phylogenetic tree for 154 flatfish individuals reconstructed in MrBayes based on the concatenated dataset with the best-fitted partitioning scheme and substitution model. The shaded bar on the right defines five major monophyletic groups inferred on the phylogeny. Arrow indicates the potential new species in the genus *Platichthys*.

Fig. 2. Collecting sites of the voucher specimens for *Hippoglossoides* species in the Pacific and Arctic oceans. The phylogenetic tree is extracted from the complete BEAST tree in Fig. S2.

Fig. 3. Four topological hypotheses tested for the clade with Hippoglossinae (shown in red color). Log Bayesian factors (log *BF*) represent the difference between log-marginal likelihoods obtained in Stepping Stone analysis between the original topology (Fig. 1; *log L* = -55821.14; log *BF* = 0) and the model with A, B, C, and D topologies. In all four tested topologies, species *L. punctatissima* was manually included into the monophyletic group with *L. ferruginea* and *L. proboscidea* (see more details in the text).

Fig. 4. Both RAxML phylogenetic trees inferred from the individual loci (A) and *BEAST species tree (B) show discrepancies in the modern classification of the family Pleuronectidae. Branch coloration represents the tribes and subfamilies accepted in Nelson et al. (2016). In the *BEAST analysis, the mitochondrial genes (*) shared the same clock and tree models, but substitution models were unlinked across all loci (see discussion in the text).

Fig. 5. Ancestral state reconstructions of abdominal (left) and caudal (right) vertebra numbers. Numbers represent ancestral node IDs. Exact estimates and their 95% confidence intervals for all ancestral nodes are provided in Table S4. *C. herzensteini* and *H. robustus* were excluded from the analysis due to their questionable validity.

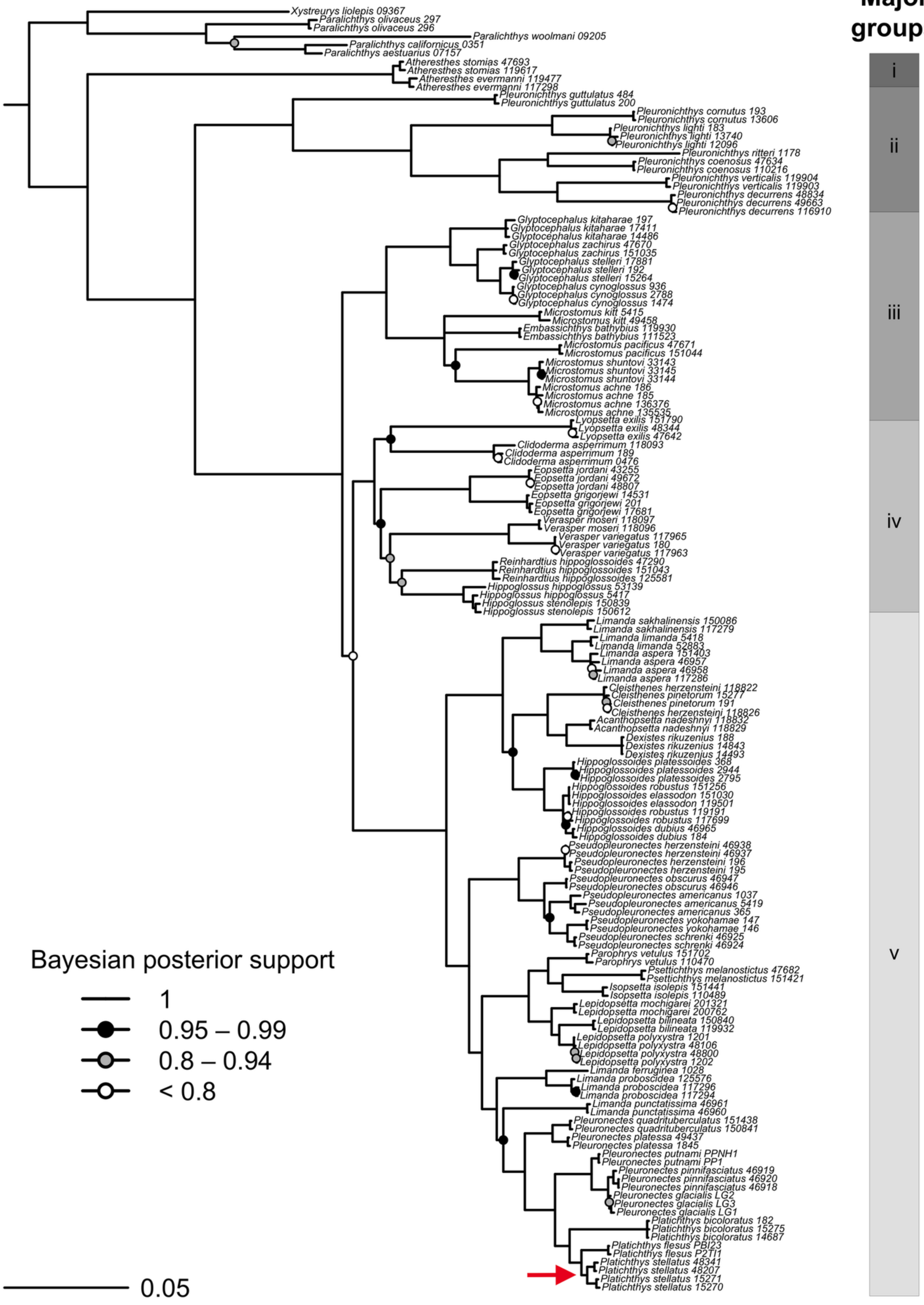
Major groups
i
ii
iii
iv
v
Xystreurys liolepis 09367
Paralichthys olivaceus 297
Paralichthys olivaceus 296
Paralichthys woolmani 09205
Paralichthys californicus 0351
Paralichthys aestuarius 07157
Atheresthes stomias 47693
Atheresthes stomias 119617
Atheresthes evermanni 119477
Atheresthes evermanni 117298
Pleuronichthys guttulatus 484
Pleuronichthys guttulatus 200
Pleuronichthys cornutus 193
Pleuronichthys cornutus 13606
Pleuronichthys lighti 183
Pleuronichthys lighti 13740
Pleuronichthys lighti 12096
Pleuronichthys ritteri 1178
Pleuronichthys coenosus 47634
Pleuronichthys coenosus 110216
Pleuronichthys verticalis 119904
Pleuronichthys verticalis 119903
Pleuronichthys decurrens 48834
Pleuronichthys decurrens 49663
Pleuronichthys decurrens 116910
Glyptocephalus kitaharae 197
Glyptocephalus kitaharae 17411
Glyptocephalus kitaharae 14486
Glyptocephalus zachirus 47670
Glyptocephalus zachirus 151035
Glyptocephalus stelleri 17881
Glyptocephalus stelleri 192
Glyptocephalus stelleri 15264
Glyptocephalus cynoglossus 936
Glyptocephalus cynoglossus 2788
Glyptocephalus cynoglossus 1474
Microstomus kitt 5415
Microstomus kitt 49458
Embassichthys bathybius 119930
Embassichthys bathybius 111523
Microstomus pacificus 47671
Microstomus pacificus 151044
Microstomus shuntovi 33143
Microstomus shuntovi 33145
Microstomus shuntovi 33144
Microstomus achne 186
Microstomus achne 185
Microstomus achne 136376
Microstomus achne 135535
Lyopsetta exilis 151790
Lyopsetta exilis 48344
Lyopsetta exilis 47642
Clidoderma asperrimum 118093
Clidoderma asperrimum 189
Clidoderma asperrimum 0476
Eopsetta jordani 43255
Eopsetta jordani 49672
Eopsetta jordani 48807
Eopsetta grigorjewi 14531
Eopsetta grigorjewi 201
Eopsetta grigorjewi 17681
Verasper moseri 118097
Verasper moseri 118096
Verasper variegatus 117965
Verasper variegatus 180
Verasper variegatus 117963
Reinhardtius hippoglossoides 47290
Reinhardtius hippoglossoides 151043
Reinhardtius hippoglossoides 125581
Hippoglossus hippoglossus 53139
Hippoglossus hippoglossus 5417
Hippoglossus stenolepis 150839
Hippoglossus stenolepis 150612
Limanda sakhalinensis 150086
Limanda sakhalinensis 117279
Limanda limanda 5418
Limanda limanda 52883
Limanda aspera 151403
Limanda aspera 46957
Limanda aspera 46958
Limanda aspera 117286
Cleisthenes herzensteini 118822
Cleisthenes pinetorum 15277
Cleisthenes pinetorum 191
Cleisthenes herzensteini 118826
Acanthopsetta nadeshnyi 118832
Acanthopsetta nadeshnyi 118829
Dexistes rikuzenius 188
Dexistes rikuzenius 14843
Dexistes rikuzenjus 14493
Hippoglossoides platessoides 368
Hippoglossoides platessoides 2944
Hippoglossoides platessoides 2795
Hippoglossoides robustus 151256
Hippoglossoides elassodon 151030
Hippoglossoides elassodon 119501
Hippoglossoides robustus 119191
Hippoglossoides robustus 117699
Hippoglossoides dubius 46965
Hippoglossoides dubius 184
Pseudopleuronectes herzensteini 46938
Pseudopleuronectes herzensteini 46937
Pseudopleuronectes herzensteini 196
Pseudopleuronectes herzensteini 195
Pseudopleuronectes obscurus 46947
Pseudopleuronectes obscurus 46946
Pseudopleuronectes americanus 1037
Pseudopleuronectes americanus 5419
Pseudopleuronectes americanus 365
Pseudopleuronectes yokohamae 147
Pseudopleuronectes yokohamae 146
Pseudopleuronectes schrenki 46925
Pseudopleuronectes schrenki 46924
Parophrys vetulus 151702
Parophrys vetulus 110470
Psettichthys melanostictus 47682
Psettichthys melanostictus 151421
Isopsetta isolepis 151441
Isopsetta isolepis 110489
Lepidopsetta mochigarei 201321
Lepidopsetta mochigarei 200762
Lepidopsetta bilineata 150840
Lepidopsetta bilineata 119932
Lepidopsetta polyxystra 1201
Lepidopsetta polyxystra 48106
Lepidopsetta polyxystra 48800
Lepidopsetta polyxystra 1202
Limanda ferruginea 1028
Limanda proboscidea 125576
Limanda proboscidea 117296
Limanda proboscidea 117294
Limanda punctatissima 46961
Limanda punctatissima 46960
Pleuronectes quadrituberculatus 151438
Pleuronectes quadrituberculatus 150841
Pleuronectes platessa 49437
Pleuronectes platessa 1845
Pleuronectes putnami PPNH1
Pleuronectes putnami PP1
Pleuronectes pinnifasciatus 46919
Pleuronectes pinnifasciatus 46920
Pleuronectes pinnifasciatus 46918
Pleuronectes glacialis LG2
Pleuronectes glacialis LG3
Pleuronectes glacialis LG1
Platichthys bicoloratus 182
Platichthys bicoloratus 15275
Platichthys bicoloratus 14687
Platichthys flesus PBI23
Platichthys flesus P2TI1
Platichthys stellatus 48341
Platichthys stellatus 48207
Platichthys stellatus 15271
Platichthys stellatus 15270
Bayesian posterior support
1
0.95 – 0.99
0.8 – 0.94
< 0.8
0.05

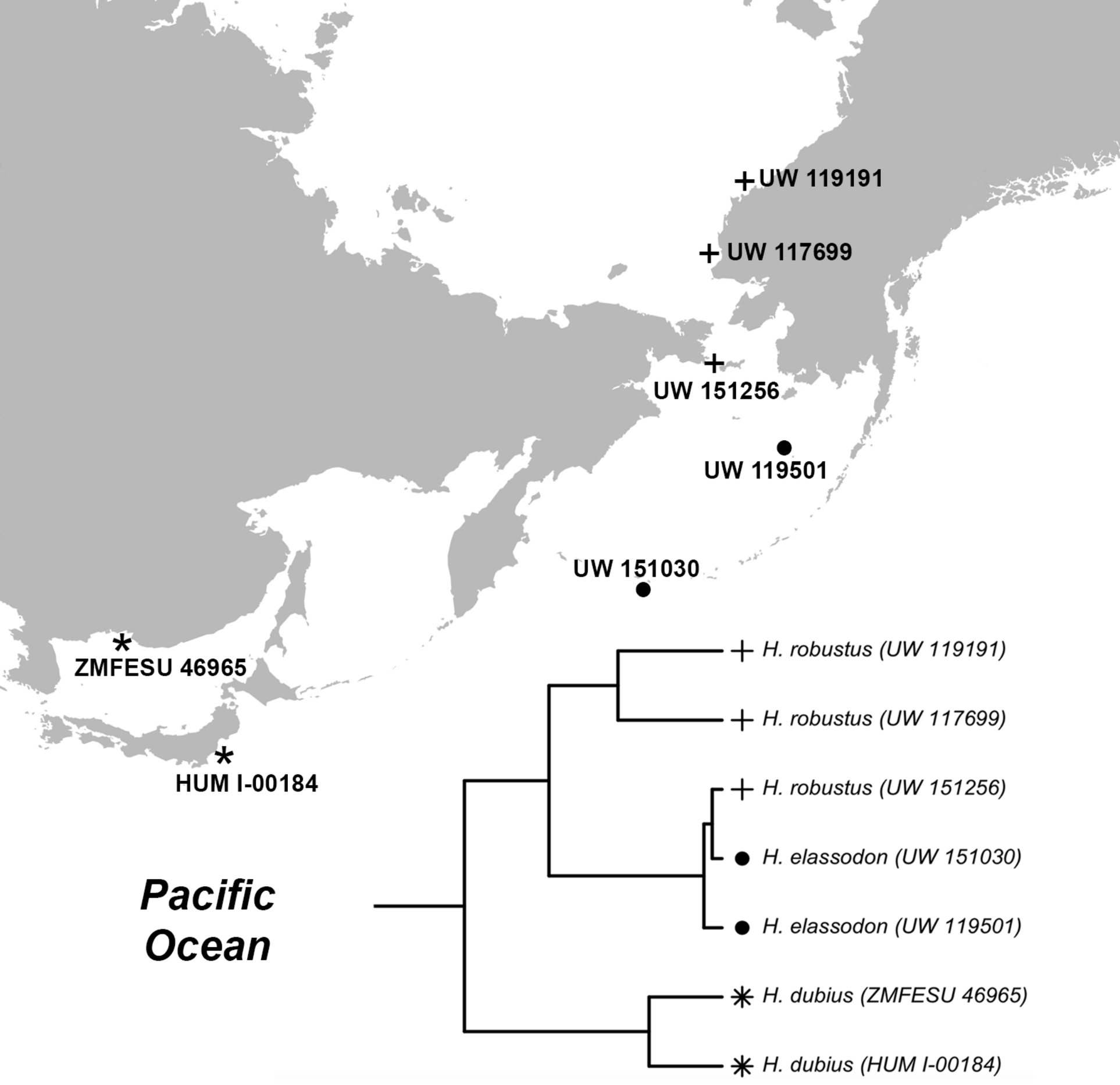
UW 119191
UW 117699
UW 151256
UW 119501
UW 151030
ZMFESU 46965
HUM I-00184
Pacific Ocean
H. robustus (UW 119191)
H. robustus (UW 117699)
H. robustus (UW 151256)
H. elassodon (UW 151030)
H. elassodon (UW 119501)
H. dubius (ZMFESU 46965)
H. dubius (HUM I-00184)

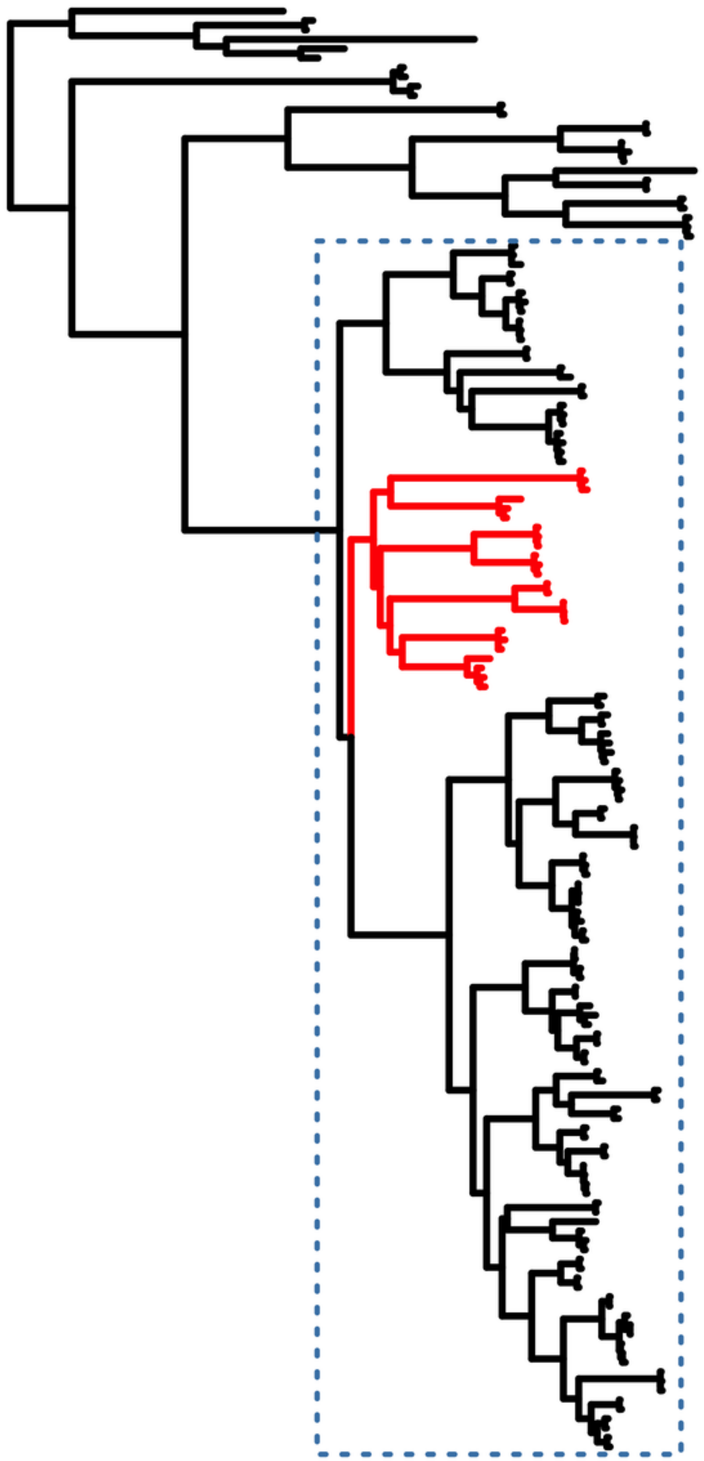

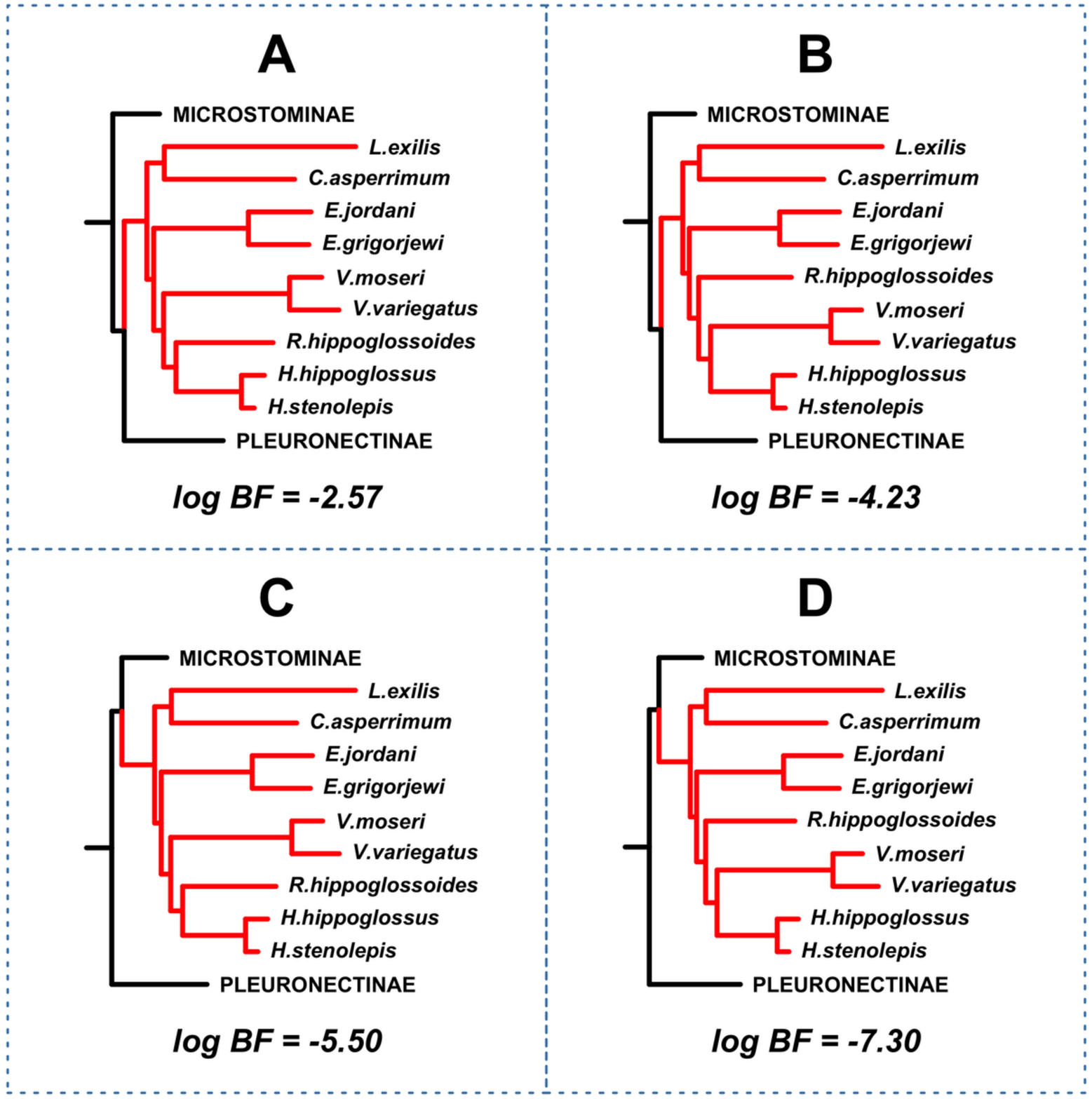
A
MICROSTOMINAE
L.exilis
C.asperrimum
E.jordani
E.grigorjewi
V.moseri
V.variegatus
R.hippoglossoides
H.hippoglossus
H.stenolepis
PLEURONECTINAE
log BF = -2.57
B
MICROSTOMINAE
L.exilis
C.asperrimum
E.jordani
E.grigorjewi
R.hippoglossoides
V.moseri
V.variegatus
H.hippoglossus
H.stenolepis
PLEURONECTINAE
log BF = -4.23
C
MICROSTOMINAE
L.exilis
C.asperrimum
E.jordani
E.grigorjewi
V.moseri
V.variegatus
R.hippoglossoides
H.hippoglossus
H.stenolepis
PLEURONECTINAE
log BF = -5.50
D
MICROSTOMINAE
L.exilis
C.asperrimum
E.jordani
E.grigorjewi
R.hippoglossoides
V.moseri
V.variegatus
H.hippoglossus
H.stenolepis
PLEURONECTINAE
log BF = -7.30

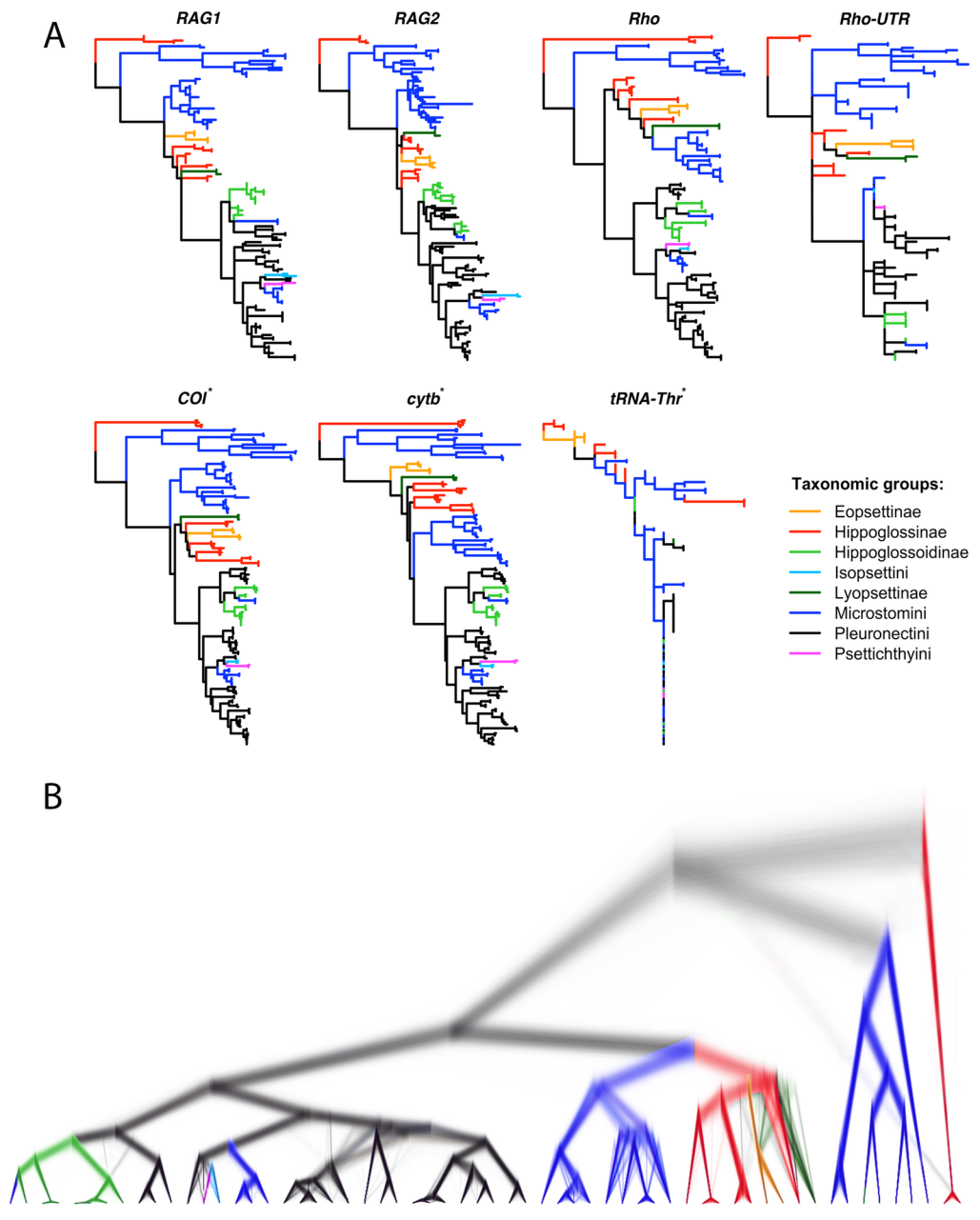
A
RAG1
RAG2
Rho
Rho-UTR
COI*
cytb*
tRNA-Thr*
Taxonomic groups:
Eopsettinae
Hippoglossinae
Hippoglossoidinae
Isopsettini
Lyopsettinae
Microstomini
Pleuronectini
Psettichthyini
B

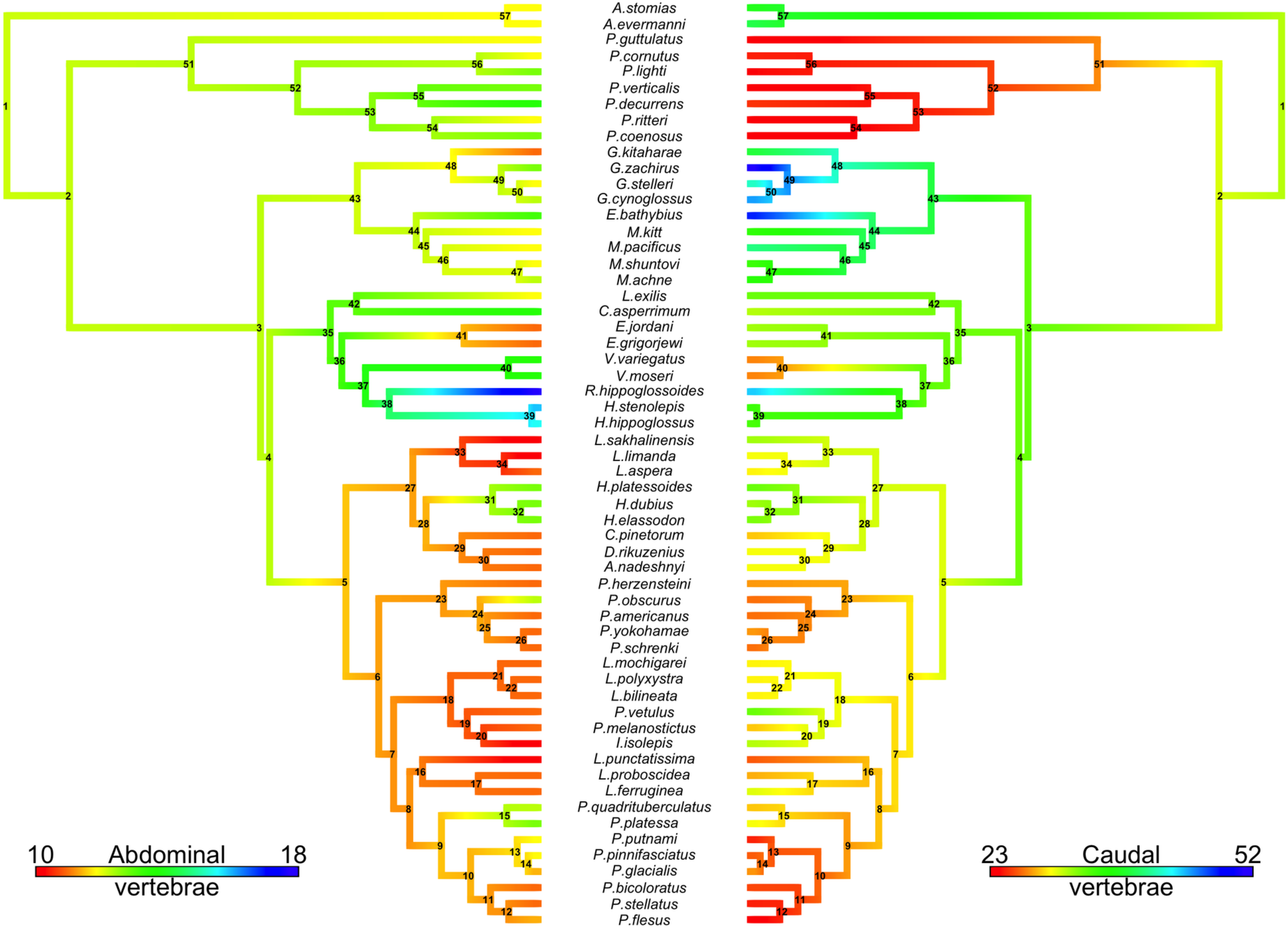
A.stomias
A.evermanni
P.guttulatus
P.cornutus
P.lighti
P.verticalis
P.decurrens
P.ritteri
P.coenosus
G.kitaharae
G.zachirus
G.stelleri
G.cynoglossus
E.bathybius
M.kitt
M.pacificus
M.shuntovi
M.achne
L.exilis
C.asperrimum
E.jordani
E.grigorjewi
V.variegatus
V.moseri
R.hippoglossoides
H.stenolepis
H.hippoglossus
L.sakhalinensis
L.limanda
L.aspera
H.platessoides
H.dubius
H.elassodon
C.pinetorum
D.rikuzenius
A.nadeshnyi
P.herzensteini
P.obscurus
P.americanus
P.yokohamae
P.schrenki
L.mochigarei
L.polyxystra
L.bilineata
P.vetulus
P.melanostictus
I.isolepis
L.punctatissima
L.proboscidea
L.ferruginea
P.quadrituberculatus
P.platessa
P.putnami
P.pinnifasciatus
P.glacialis
P.bicoloratus
P.stellatus
P.flesus
10 Abdominal 18
vertebrae
23 Caudal 52
vertebrae

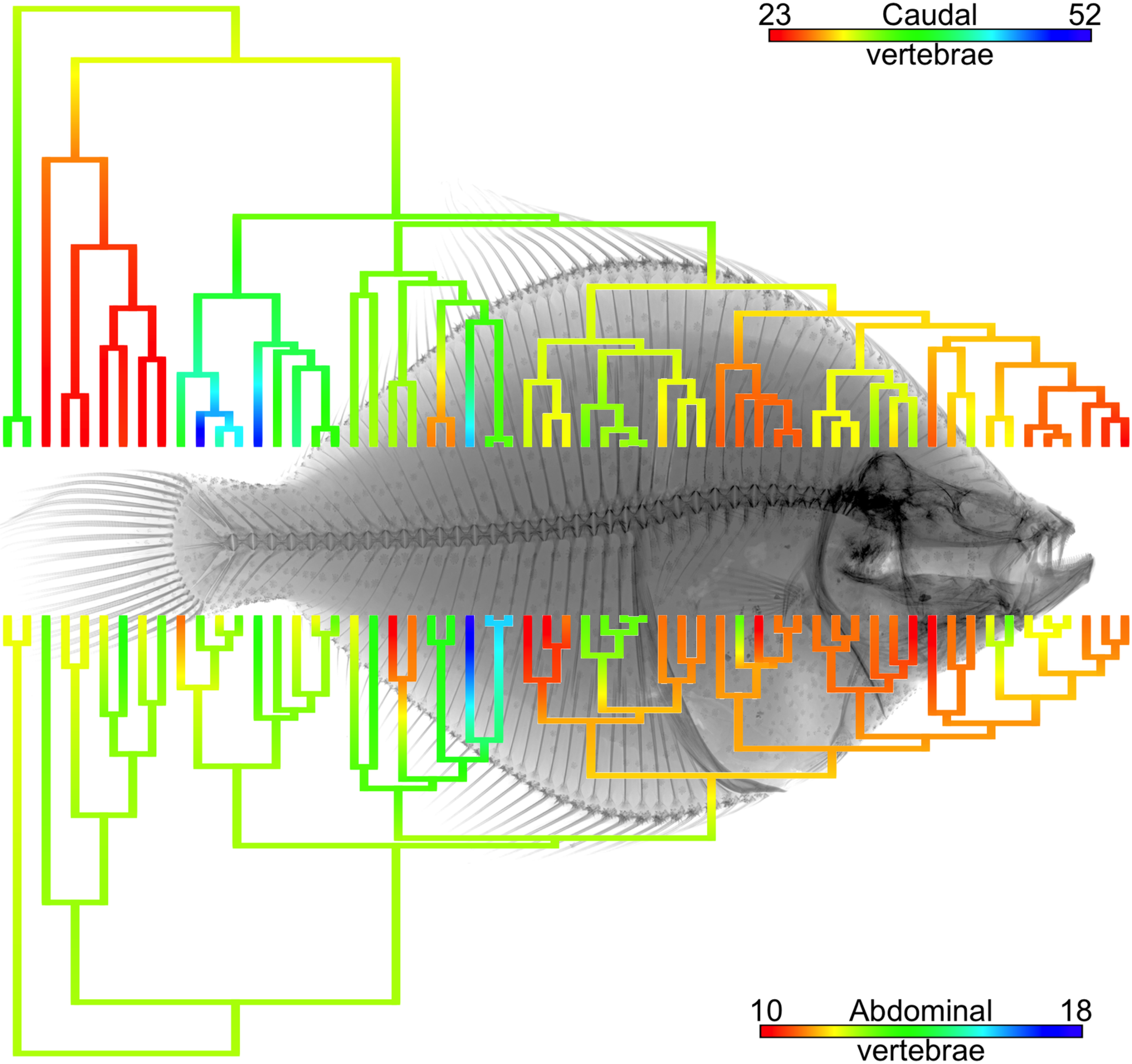
23
Caudal
52
vertebrae
10
Abdominal
18
vertebrae